CONFIDENTIAL

RM A9E05

NACA RM A9E05

NACA

RESEARCH MEMORANDUM

THE AERODYNAMIC CHARACTERISTICS THROUGHOUT THE SUBSONIC SPEED RANGE OF A THIN, SHARP-EDGED HORIZONTAL TAIL OF ASPECT RATIO 4 EQUIPPED WITH A CONSTANT-CHORD ELEVATOR

By Angelo Bandettini and Verlin D. Reed

Ames Aeronautical Laboratory
Moffett Field, Calif.

NATIONAL ADVISORY COMMITTEE FOR AERONAUTICS

WASHINGTON
June 30, 1949

CONFIDENTIAL

NATIONAL ADVISORY COMMITTEE FOR AERONAUTICS

RESEARCH MEMORANDUM

THE AERODYNAMIC CHARACTERISTICS THROUGHOUT THE SUBSONIC SPEED RANGE OF A THIN, SHARP-EDGED HORIZONTAL TAIL OF ASPECT RATIO 4 EQUIPPED WITH A CONSTANT-CHORD ELEVATOR

By Angelo Bandettini and Verlin D. Reed

SUMMARY

Wind-tunnel tests have been made of a semispan model of a horizontal tail of aspect ratio 4 and taper ratio 0.5 equipped with a full-span constant-chord elevator having an area equal to 20 percent of the total semispan-tail area. The horizontal tail was not swept and the profile was a sharp-edged, faired double wedge with a thickness-chord ratio of 0.042. Lift, drag, and pitching-moment data are presented for a Reynolds number of 2,000,000 at Mach numbers from 0.20 to 0.94.

At small angles of attack and small elevator deflections, the effect of compressibility on the effectiveness of the elevator in producing lift was small at Mach numbers less than 0.60. There was a gradual increase in effectiveness between Mach numbers of 0.60 and 0.90 to a value equal to 146 percent of the low-speed value. At higher Mach numbers the effectiveness decreased slightly to a value at a Mach number of 0.94 equal to 127 percent of the low-speed value. The variation of lift coefficient with elevator deflection was not linear, the effectiveness being lower for deflections from 0° to 2° than for deflections from 2° to 4°. Neither the magnitude nor extent of this nonlinearity in effectiveness at small elevator deflections was aggravated by compressibility.

INTRODUCTION

Recent investigations have indicated several wing plan forms, wing sections, and wing-body-tail combinations suitable for flight at supersonic speeds. One such lifting surface, a thin, sharp-edged wing without sweep of aspect ratio 4 and taper ratio 0.5, has been

the subject of an investigation in the Ames 12-foot pressure wind tunnel. The aim of the investigation was to determine the aerodynamic characteristics of such a wing plan form throughout the range of subsonic Mach numbers up to 0.94. Various phases of the investigation have been reported in references 1, 2, 3, and 4. Application of the data of these references to a wing-body-tail combination indicated the possibility of obtaining adequate longitudinal control throughout the speed range by using either an all-movable stabilizer or an adjustable stabilizer with an elevator. To provide data on the effectiveness of an elevator applied to such a plan form, the model previously tested as a wing has been tested as a horizontal tail with a full-span elevator. The tests were conducted at a constant Reynolds number of 2,000,000 at Mach numbers from 0.20 to 0.94.

COEFFICIENTS AND SYMBOLS

The following coefficients are used in this report:

C_L lift coefficient $\left(\frac{\text{lift}}{qS}\right)$

C_D drag coefficient $\left(\frac{\text{drag}}{qS}\right)$

C_m pitching-moment coefficient about quarter-chord point of the mean aerodynamic chord $\left(\frac{\text{pitching moment}}{qS\bar{c}}\right)$

The following symbols are used in this report:

a speed of sound, feet per second

b twice model semispan, feet

c local chord, feet

$\bar{c}$ mean aerodynamic chord, chord through centroid of semispan plan-form area $\left(\frac{\int_0^{b/2} c^2\,dy}{\int_0^{b/2} c\,dy}\right)$, feet

M Mach number $\left(\frac{V}{a}\right)$

q free-stream dynamic pressure $\left(\frac{\rho V^2}{2}\right)$, pounds per square foot

R	Reynolds number $\left(\frac{\rho V \bar{c}}{\mu}\right)$
S	area of semispan tail, square feet
V	airspeed, feet per second
y	distance from plane of symmetry to any spanwise station, feet
α	angle of attack of tail-chord plane, degrees
δ_e	elevator deflection, positive to increase lift, degrees
μ	viscosity of air, slugs per foot-second
ρ	mass density of air, slugs per cubic foot
C_{L_α}	$\left(\frac{\partial C_L}{\partial \alpha}\right)_{\delta=0^\circ}$, measured at $\alpha=0^\circ$
$C_{L_\delta}{}^*$	$\left(\frac{C_{L_{\delta=4^\circ}} - C_{L_{\delta=0^\circ}}}{4}\right)_{\alpha=0^\circ}$
α_δ	$-\left(\frac{C_{L_\delta}{}^*}{C_{L_\alpha}}\right)_{C_L=0}$

(The subscripts outside the parenthesis indicate the factor held constant during the measurement of the parameters.)

MODEL AND APPARATUS

The tests were conducted in the Ames 12-foot pressure wind tunnel. The horizontal tail with full-span elevator used in this investigation was the same model as that used in the tests reported in reference 1. The semispan model represented a tail of aspect ratio 4 and taper ratio 0.5. The 50-percent-chord line of the tail was normal to the plane of symmetry and the airfoil profile was a sharp-edged, symmetrical, faired double wedge with a thickness-chord ratio of 0.042. The constant-chord elevator had an area equal to 20 percent of the total semispan tail area. The unsealed gap between the elevator and the tail was 0.015 inch. Dimensions of the model are given in figure 1. The semispan model was mounted vertically in the tunnel as shown in figure 2. The leading-edge flap with which the model was equipped remained undeflected throughout the present series of tests and all surface roughness

associated with the leading-edge flap and its angle brackets was minimized by sealing the gap and smoothing the surface. The elevator was attached to the tail by hinges and rigidly held in position by steel angle plates. Angular distortion of the elevator due to aerodynamic loads was negligible.

CORRECTIONS TO DATA

The data of this investigation have been corrected for tunnel-wall interference, constriction due to the tunnel walls, and model-support tare forces. The method of reference 5 was used in correcting the data for tunnel-wall interference. The following corrections were added:

$$\Delta\alpha = 0.363\ C_L$$

$$\Delta C_D = 0.0056\ C_L^2$$

$$\Delta C_m = 0$$

Corrections to the data for constriction effects of the tunnel walls have been evaluated by the method of reference 6. The magnitude of these corrections as applied to Mach number and to dynamic pressure (measured with the tunnel empty) is illustrated by the following table:

Corrected Mach number	Uncorrected Mach number	$\frac{q_{corrected}}{q_{uncorrected}}$[1]
0.94	0.931	1.004
.92	.915	1.003
.90	.897	1.002
.87	.868	1.002
.85	.848	1.002
.80	.799	1.001
.70	.700	1.001
.50	.500	1.001
.20	.200	1.001

[1]The values of $q_{corrected}/q_{uncorrected}$ which were presented in references 1, 3, and 4, were erroneously tabulated and were not the values used in the reduction of the data. The correct values are presented herein and are the values which were actually applied to all test data on this model.

Tare corrections due to the air forces exerted on the exposed area of the turntable were obtained from force measurements made with the model removed from the tunnel. Possible interference effects between the model and the turntable were not evaluated but they are believed to be small. The magnitude of the measured tare drag coefficient was 0.0063.

TESTS

Lift, drag, and pitching-moment data have been obtained for a range of angle of attack at a constant Reynolds number of 2,000,000 and Mach numbers from 0.20 to 0.94. For each angle of attack and Mach number, tests were made with elevator deflections of 0°, 2°, 4°, 6°, 10°, 20°, and 30° except at a Mach number of 0.94 where the maximum elevator deflection was limited to 20°. At low speeds, the angle-of-attack range was from -15° to 15°, but at Mach numbers above 0.85 the range was limited by tunnel power and model strength.

RESULTS AND DISCUSSION

Lift, drag, and pitching-moment characteristics as a function of angle of attack are presented in figures 3 to 11, inclusive, for elevator deflections of 0°, 2°, 4°, 6°, 10°, 20°, and 30° at Mach numbers of 0.20, 0.50, 0.70, 0.80, 0.85, 0.87, 0.90, 0.92, and 0.94. Since the tail profile is symmetrical, the data presented in these figures for positive elevator deflections can be used to indicate the effect of negative elevator deflections by simply reversing the algebraic signs of the coordinate axes. The variation of lift coefficient with elevator deflection for various Mach numbers is shown in figure 12 and the lift data are plotted in figures 13 and 14 as a function of Mach number.

Lift Characteristics

Stabilizer effectiveness.- The aerodynamic characteristics of the horizontal tail with the elevator neutral (figs. 3 to 11, inclusive) have been fully reported in reference 1. Despite the symmetry of the profile, the character of the stall with the elevator neutral was dependent on the algebraic sign of the angle of attack. This is especially noticeable at a Mach number of 0.80 (fig. 6) where the tail stalled abruptly with a sizable loss of lift at 8° angle of attack, but had a gentle stall with a relatively small loss of lift at about -12° angle of attack. This asymmetry may be due in part to

a small inadvertent deflection of the leading-edge flap or to differences in the surface roughness of the upper and lower surfaces as a result of the flap angle brackets. Except at the Mach number of 0.80, the variation of lift coefficient with angle of attack with the elevator neutral was nearly symmetrical about the angle of zero lift. At Mach numbers of 0.80 and 0.85 with the elevator neutral, the tail stalled abruptly with a sizable loss of lift; whereas at Mach numbers less than 0.80 the lift curve was rounded at the stall. The Mach number at which the type of stall changed was affected to some extent by the Reynolds number as can be seen from the data of reference 1.

The effect of compressibility on the lift-curve slope with the elevator neutral is shown in figure 15. The lift-curve slope increased from 0.062 to 0.095 as the Mach number increased from 0.20 to 0.94.

Elevator effectiveness.- The variation of lift coefficient with elevator deflection for various Mach numbers is shown in figure 12. At deflections between 0° and 2°, the elevator effectiveness was generally lower than for deflections between 2° and 4°. Neither the magnitude nor the extent of this reduced effectiveness at deflections near zero was aggravated by compressibility. At a Mach number of 0.20, the elevator effectiveness was approximately linear from 2° to 15° with a value of slope $\partial C_L/\partial \delta$ of 0.034. The value of $\partial C_L/\partial \delta$ predicted from thin-airfoil theory (reference 7), assuming the experimental value of tail lift-curve slope, was 0.035.

The effects of compressibility on the elevator effectiveness parameters are presented in figure 15 where $C_{L_\delta}{}^*$ and α_δ are shown as functions of Mach number. Due to the nonlinearity of the variation of the lift coefficient with elevator deflection for small elevator deflections, the effectiveness parameter $C_{L_\delta}{}^*$ was obtained as the difference in the lift coefficient due to 4° of elevator deflection divided by 4. The value of $C_{L_\delta}{}^*$ was 0.030 and was not affected by compressibility at Mach numbers less than 0.60. As the Mach number was increased to 0.90, $C_{L_\delta}{}^*$ increased to 0.044, subsequently decreasing to 0.038 at a Mach number of 0.94.

To demonstrate more clearly the effects of compressibility on the elevator effectiveness, the variation of lift coefficient with Mach number for various angles of attack of the tail with constant elevator deflections is presented in figure 13, and the variation of lift coefficient with Mach number for various elevator deflections at constant angles of attack is presented in figure 14. In figure 14, the data obtained with a positive elevator deflection and a negative angle of

attack are presented as data for negative elevator deflections at a positive angle of attack.

Drag Characteristics

The effects of elevator deflection on the drag characteristics of the horizontal tail are shown in figures 3 to 11, inclusive. At Mach numbers less than 0.80 the minimum drag coefficient was little affected by elevator deflection for deflections up to 6°. At elevator deflections greater than 6°, the minimum drag coefficient increased with increasing elevator deflection at all Mach numbers. At all Mach numbers less than 0.92, the maximum lift–drag ratio was increased slightly by small deflections of the elevator.

Pitching–Moment Characteristics

The effects of elevator deflection on the pitching–moment characteristics of the horizontal tail are presented in figure 3 to 11, inclusive. At a Mach number of 0.20, there was a marked rearward movement of the aerodynamic center starting at an angle of attack of approximately 6°. The angle of attack at which this movement started was not affected by elevator deflection. As the Mach number increased, the extent of the rearward movement was reduced and occurred at slightly smaller angles of attack. The effect of elevator deflection on the pitching–moment coefficient was strongly affected by compressibility. At a Mach number of 0.20, the pitching–moment coefficient at zero lift due to 6° of elevator deflection was −0.056. With this same elevator deflection and at a Mach number of 0.94, the pitching–moment coefficient at zero lift was −0.120, an increase of 114 percent. Similar increases in pitching–moment coefficient with increasing Mach number are apparent for all elevator deflections.

Ames Aeronautical Laboratory,
National Advisory Committee for Aeronautics,
Moffett Field, Calif.

REFERENCES

1. Johnson, Ben H., Jr.: Investigation of a Thin Wing of Aspect Ratio 4 in the Ames 12-Foot Pressure Wind Tunnel. I - Characteristics of a Plain Wing. NACA RM A8D07, 1948.

2. Johnson, Ben H., Jr., and Bandettini, Angelo: Investigation of a Thin Wing of Aspect Ratio 4 in the Ames 12-Foot Pressure Wind Tunnel. II - The Effect of Constant-Chord Leading- and Trailing-Edge Flaps on the Low-Speed Characteristics of the Wing. NACA RM A8F15, 1948.

3. Johnson, Ben H., Jr., and Demele, Fred A.: Investigation of a Thin Wing of Aspect Ratio 4 in the Ames 12-Foot Pressure Wind Tunnel. III - The Effectiveness of a Constant-Chord Aileron. NACA RM A8I17, 1948.

4. Johnson, Ben H., Jr., and Reed, Verlin D.: Investigation of a Thin Wing of Aspect Ratio 4 in the Ames 12-Foot Pressure Wind Tunnel. IV - The Effect of a Constant-Chord Leading-Edge Flap at High Subsonic Speeds. NACA RM A8K19, 1949.

5. Sivells, James C., and Deters, Owen J.: Jet-Boundary and Plan-Form Corrections for Partial-Span Models with Reflection Plane, End Plate, or no End Plate, in a Closed Circular Wind Tunnel. NACA TN 1077, 1946.

6. Herriot, John G.: Blockage Corrections for Three-Dimensional-Flow Closed-Throat Wind Tunnels, with Consideration of the Effect of Compressibility. NACA RM A7B28, 1947.

7. Allen, H. Julian: Calculation of the Chordwise Load Distribution over Airfoil Sections with Plain, Split, or Serially Hinged Trailing-Edge Flaps. NACA Rep. 634, 1938.

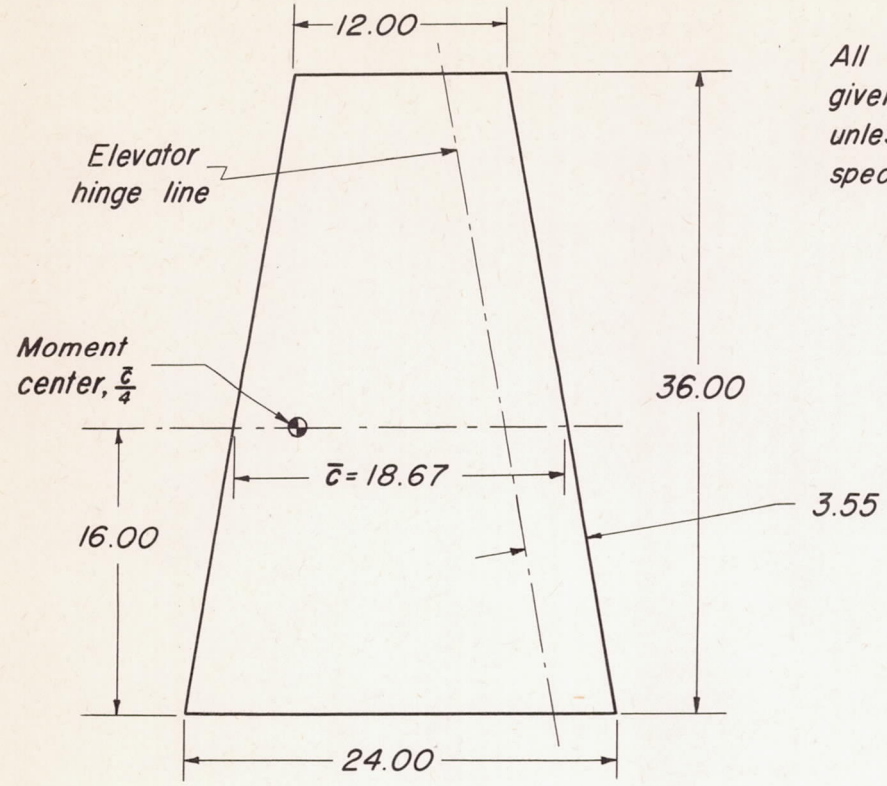

Tail plan form

Note: Leading – and trailing – edge radii are 0.005.

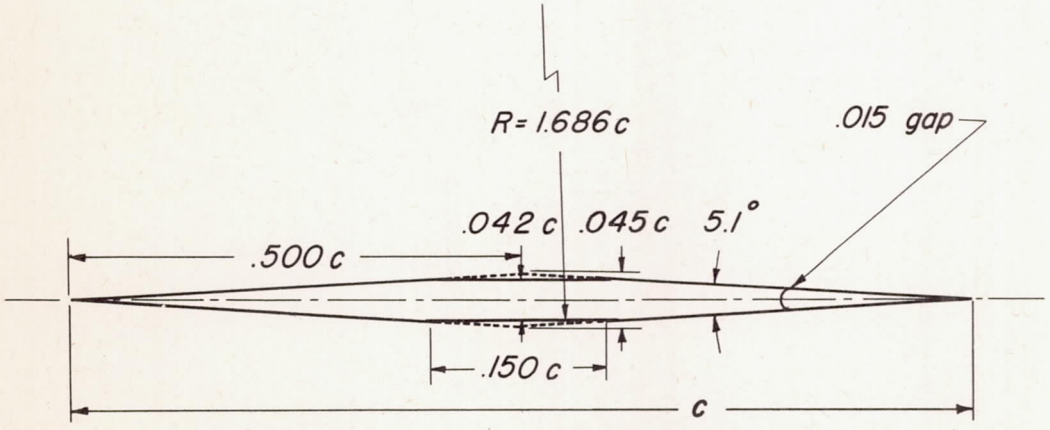

Typical section, symmetrical faired double wedge

NACA

Figure 1.– Semispan model of a horizontal tail of aspect ratio 4 tested in the Ames 12 – foot pressure wind tunnel.

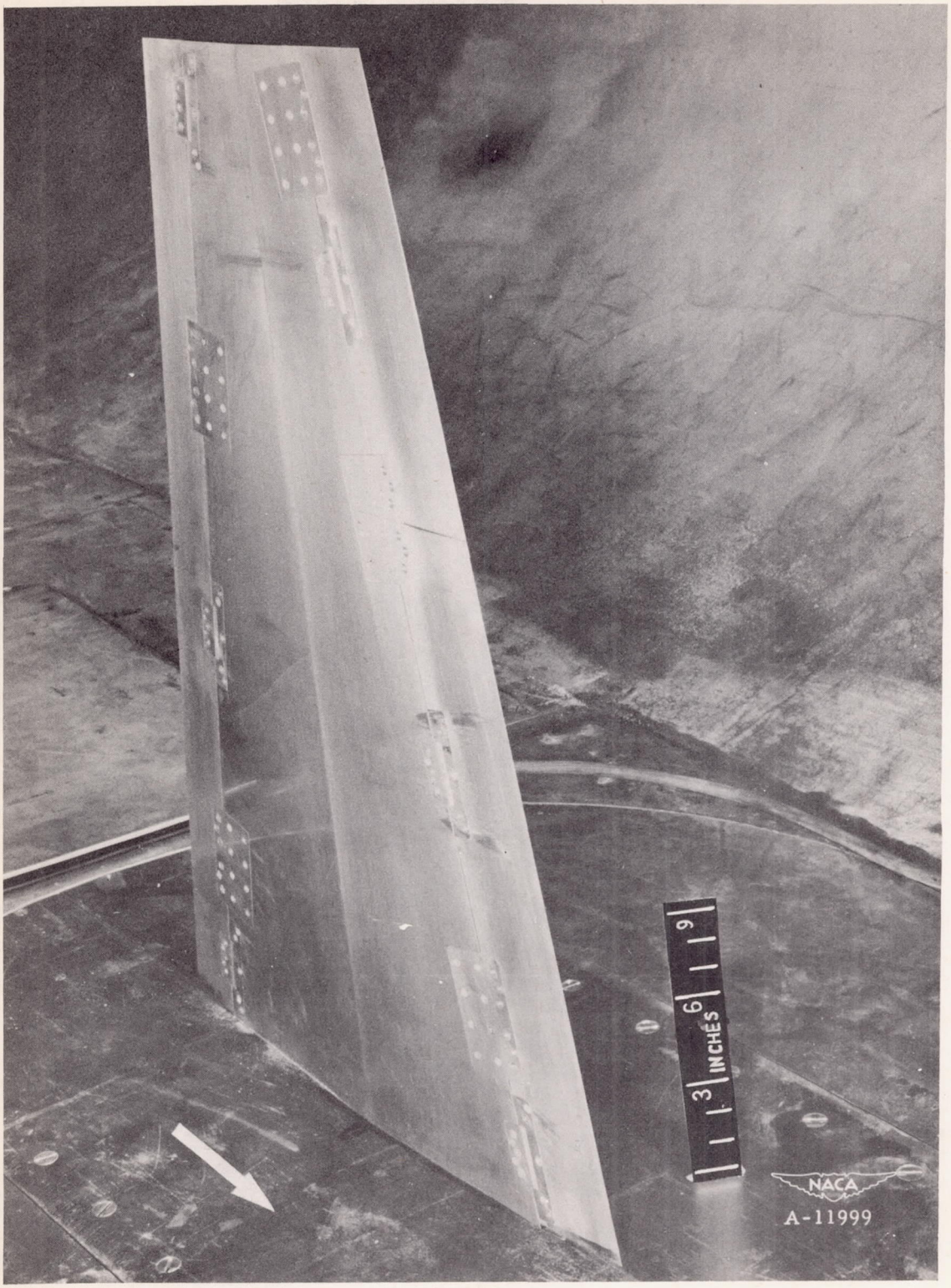

Figure 2.- Semispan model of a horizontal tail of aspect ratio 4 mounted in the Ames 12-foot pressure wind tunnel.

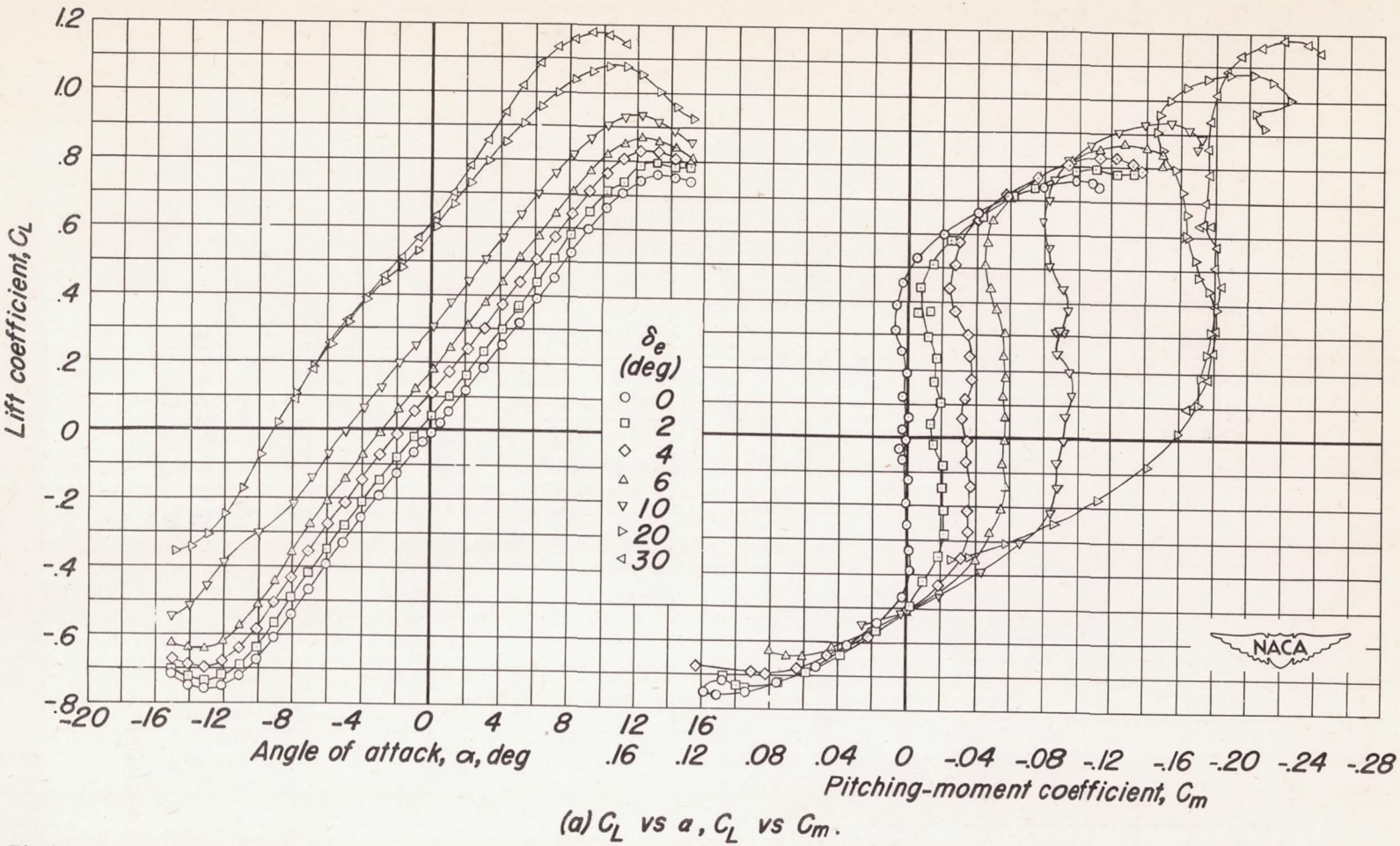

(a) C_L vs α, C_L vs C_m.

Figure 3. — The effect of elevator deflection on the aerodynamic characteristics of the tail at a Mach number of 0.20.

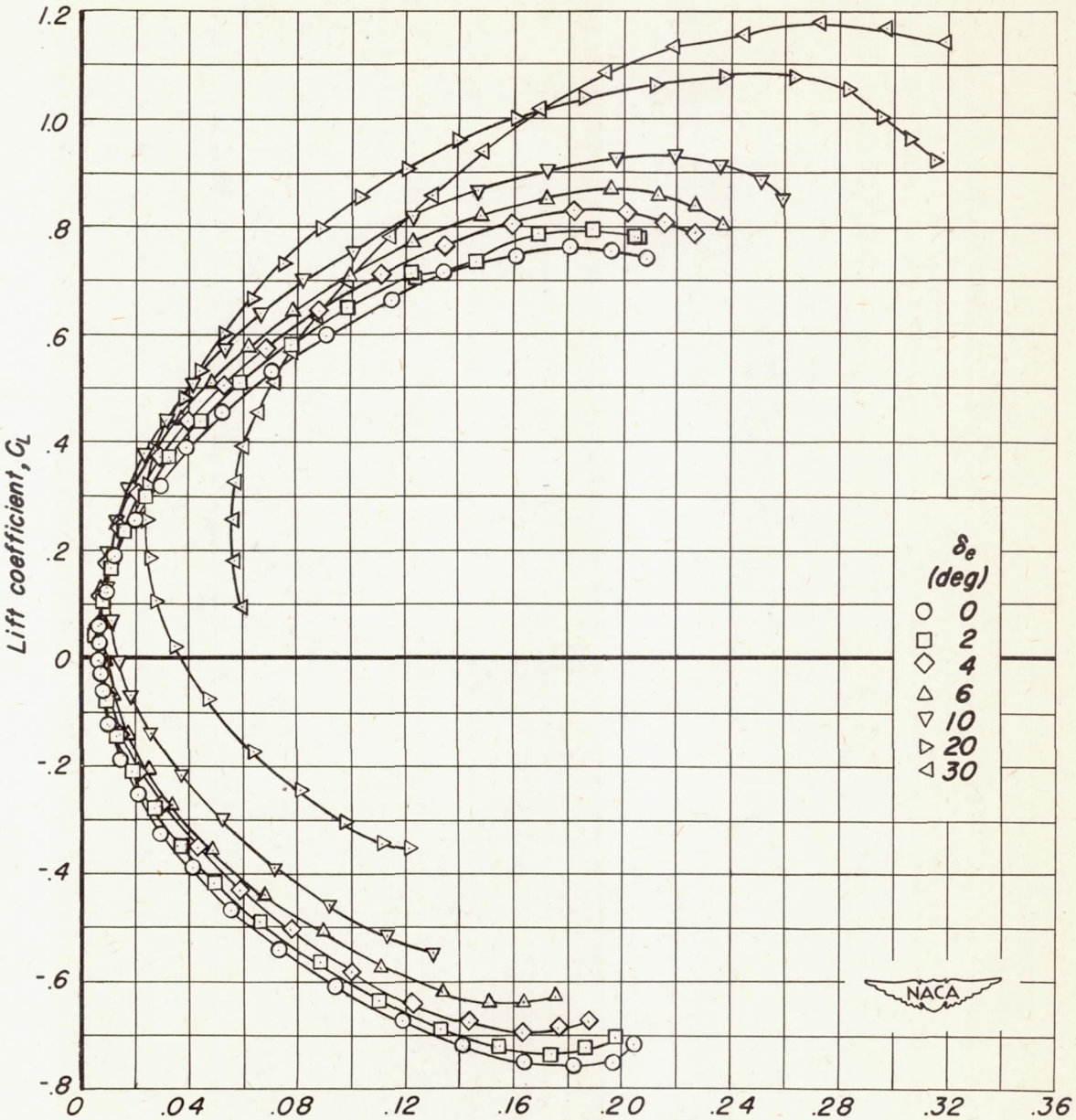

(b) C_L vs C_D.

Figure 3. — Concluded.

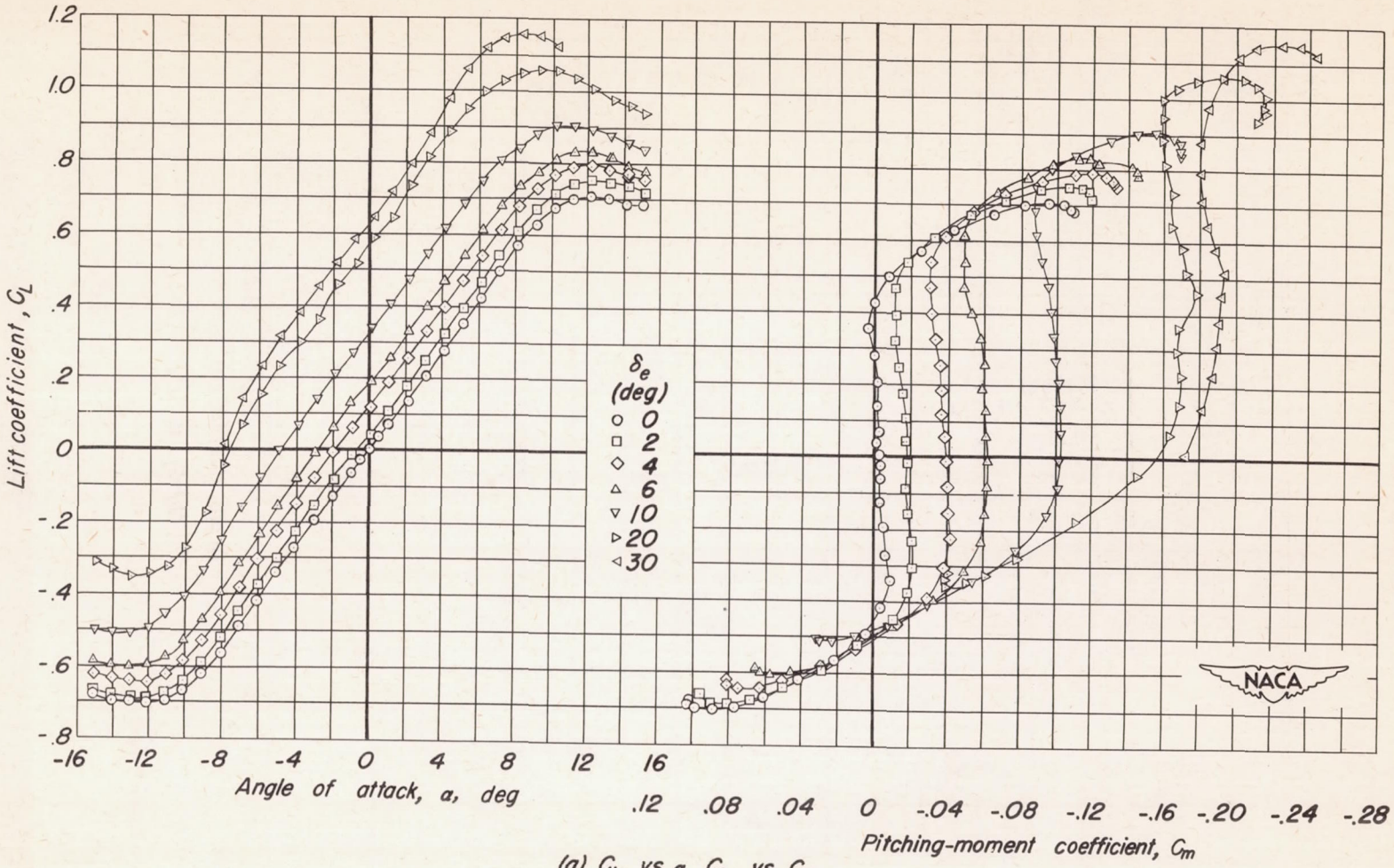

(a) C_L vs α, C_L vs C_m.

Figure 4. — The effect of elevator deflection on the aerodynamic characteristics of the tail at a Mach number of 0.50.

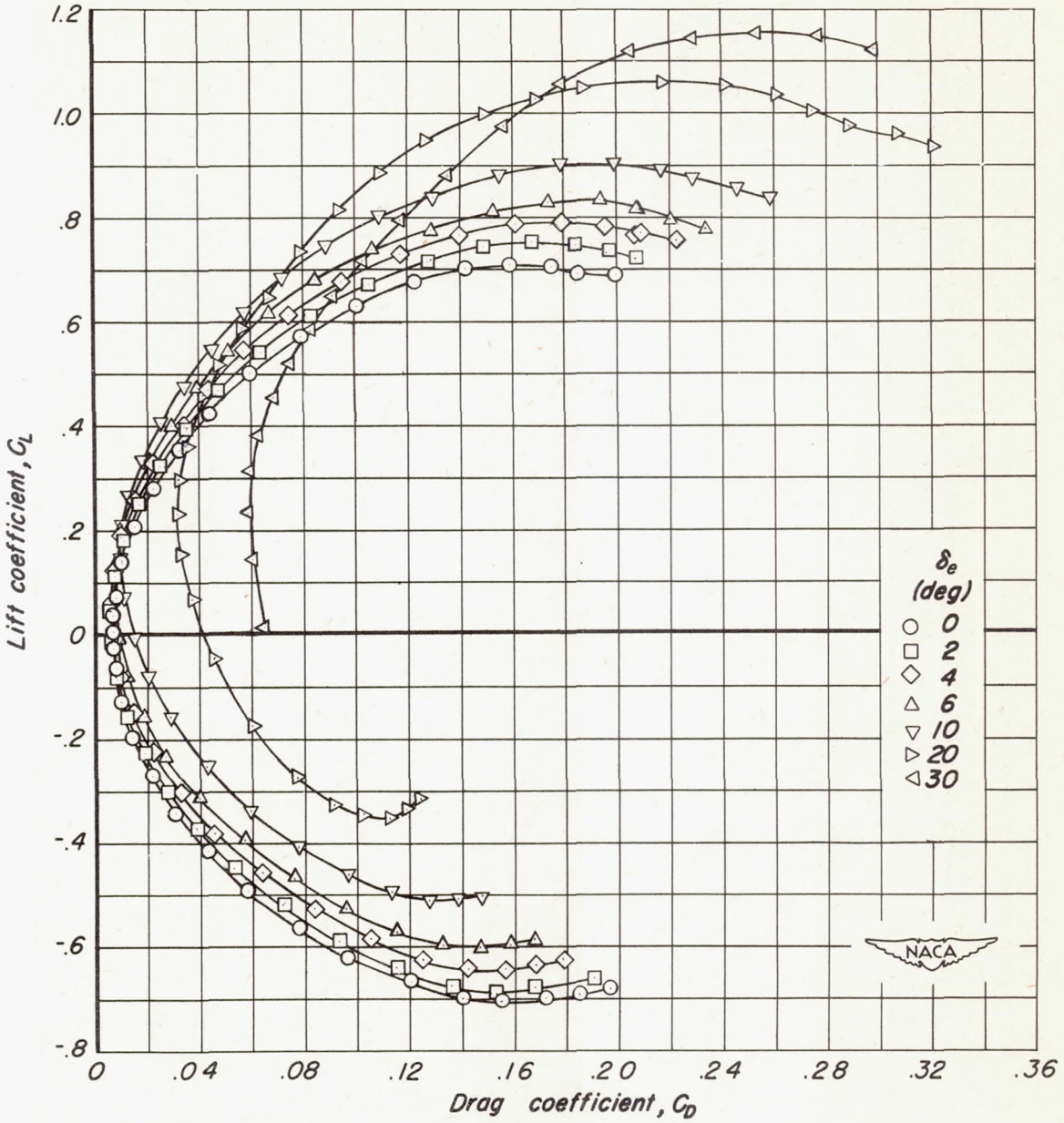

(b) C_L vs C_D.

Figure 4. — Concluded.

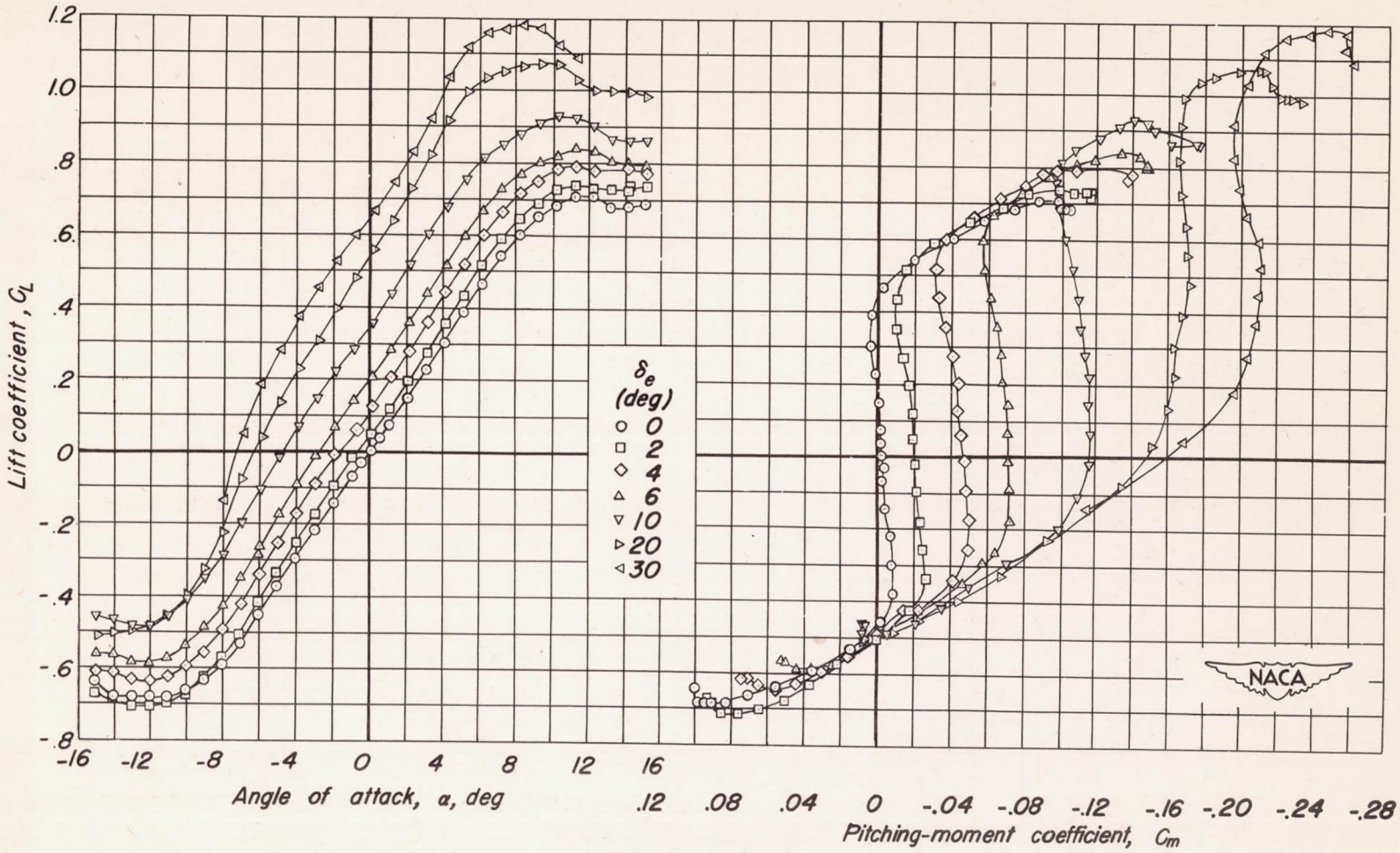

(a) C_L vs α, C_L vs C_m.

Figure 5. — The effect of elevator deflection on the aerodynamic characteristics of the tail at a Mach number of 0.70.

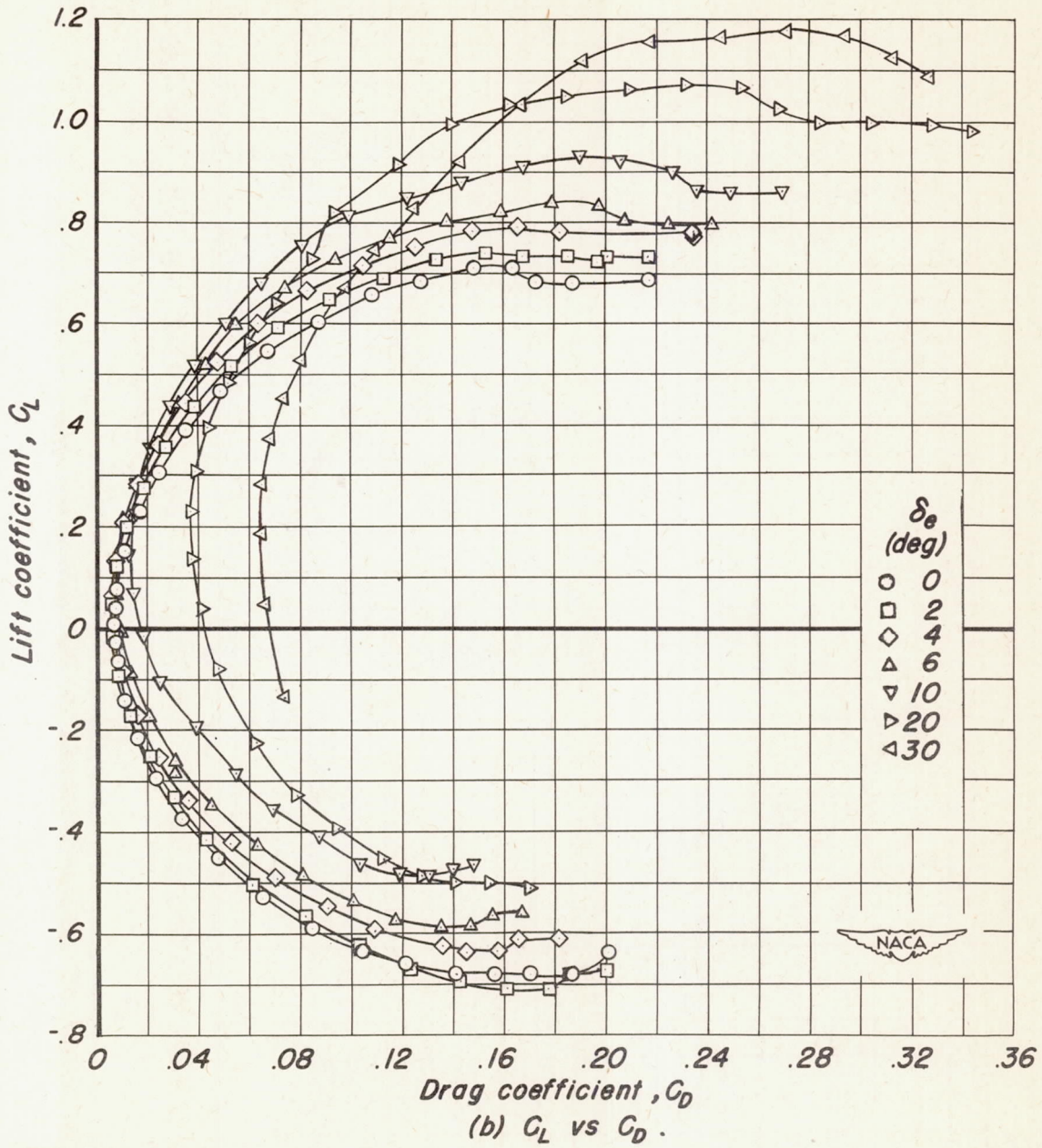

(b) C_L vs C_D.

Figure 5.—Concluded.

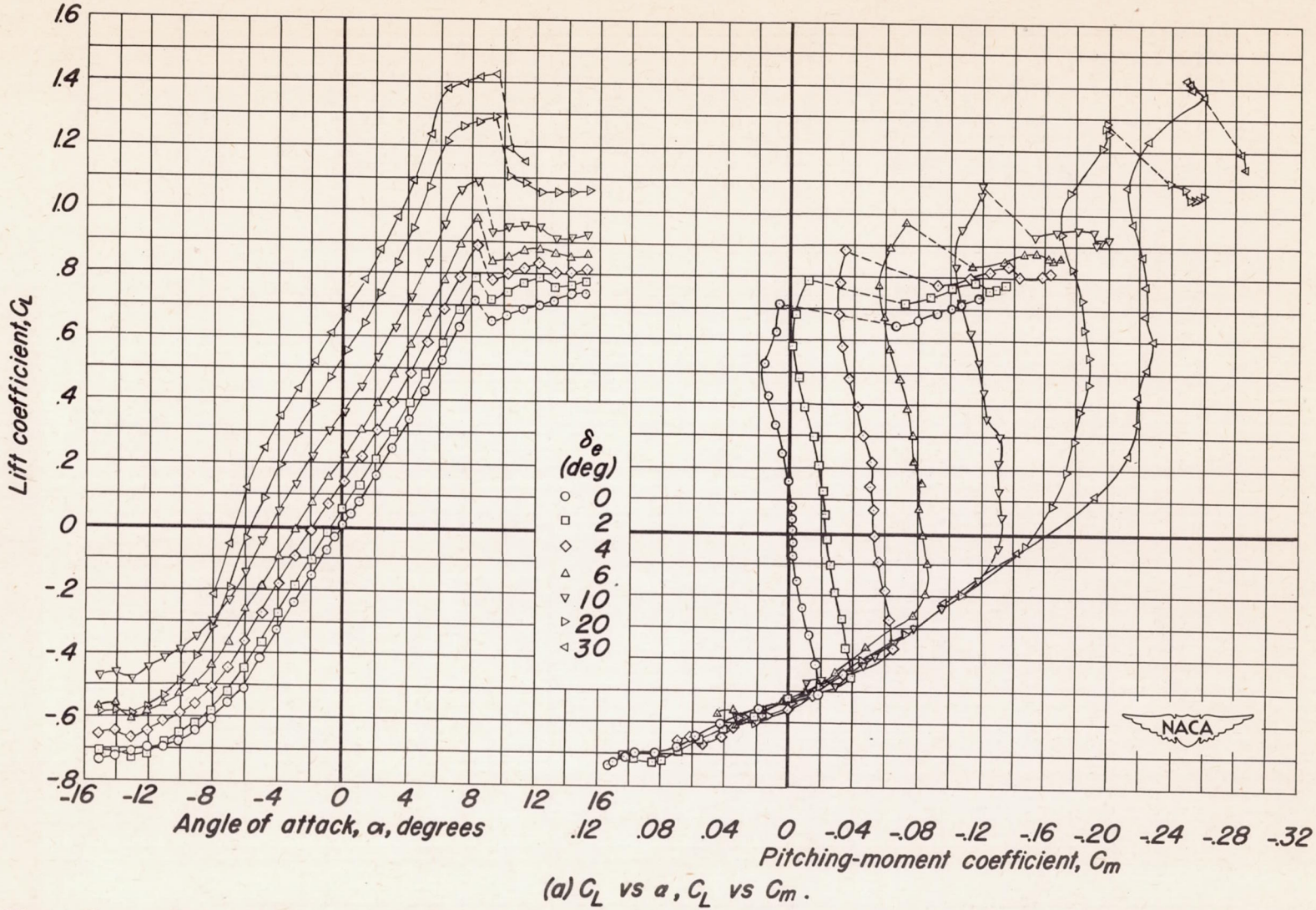

(a) C_L vs α, C_L vs C_m.

Figure 6. — The effect of elevator deflection on the aerodynamic characteristics of the tail at a Mach number of 0.80.

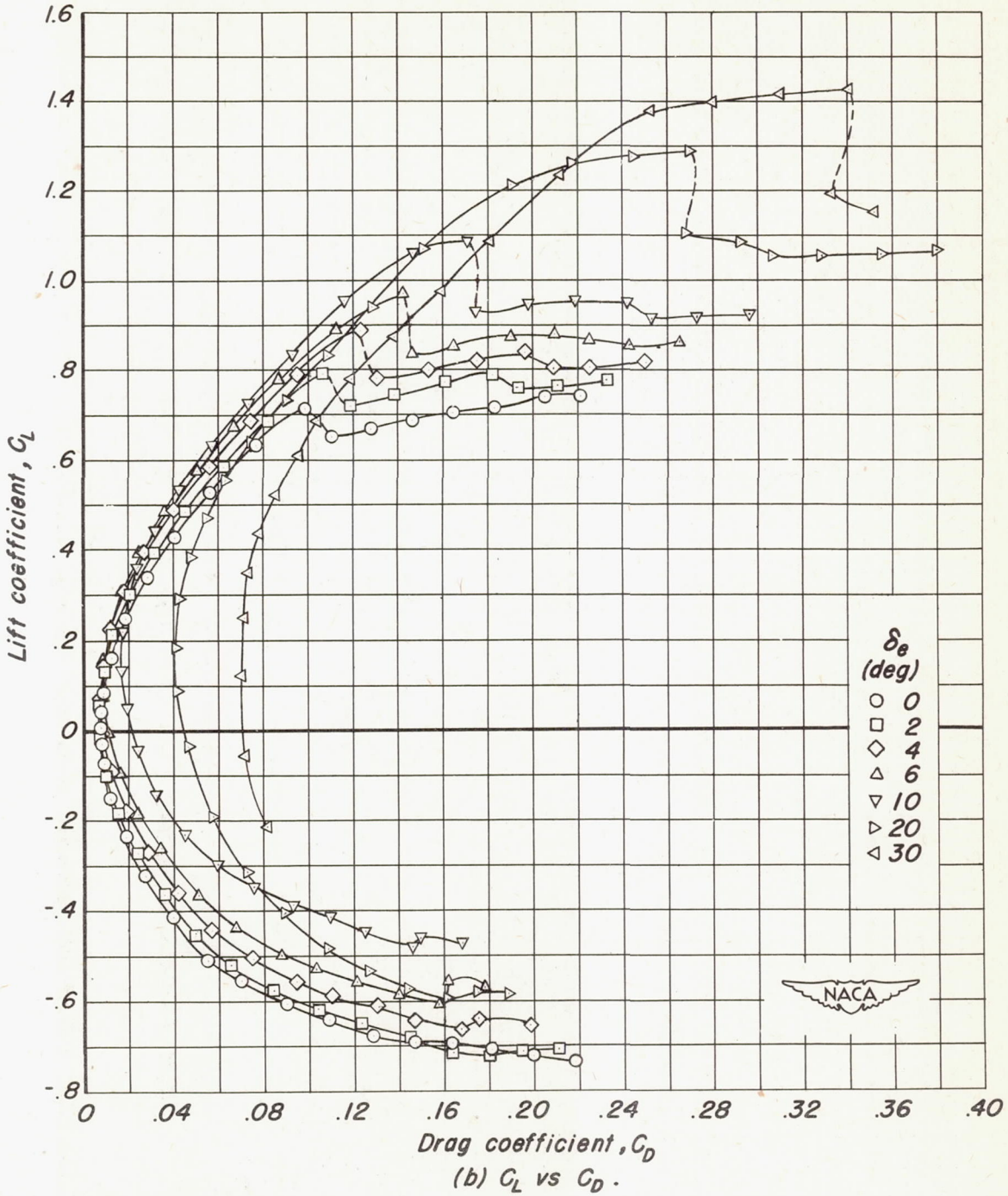

(b) C_L vs C_D.

Figure 6.—Concluded.

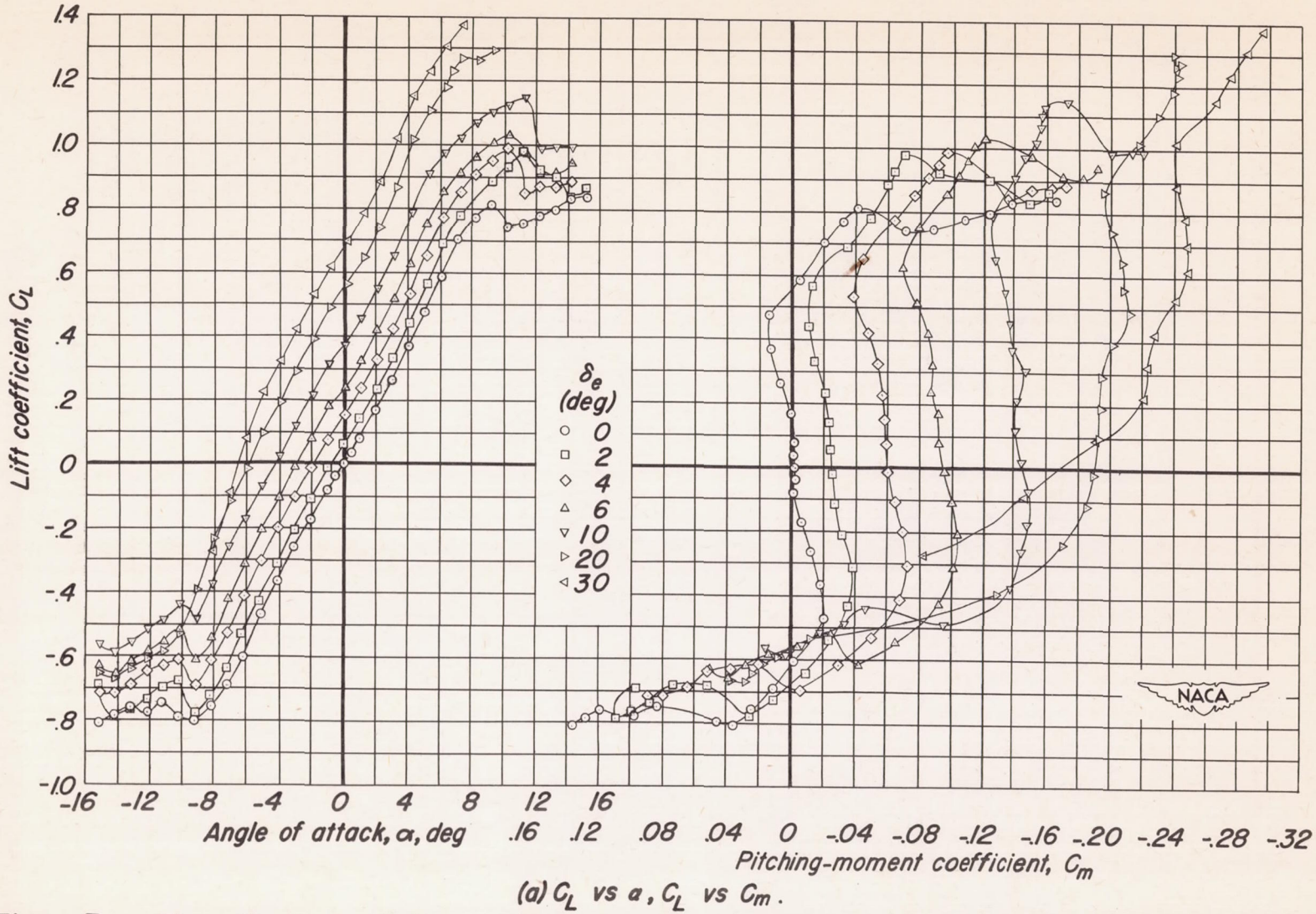

(a) C_L vs α, C_L vs C_m.

Figure 7. — The effect of elevator deflection on the aerodynamic characteristics of the tail at a Mach number of 0.85.

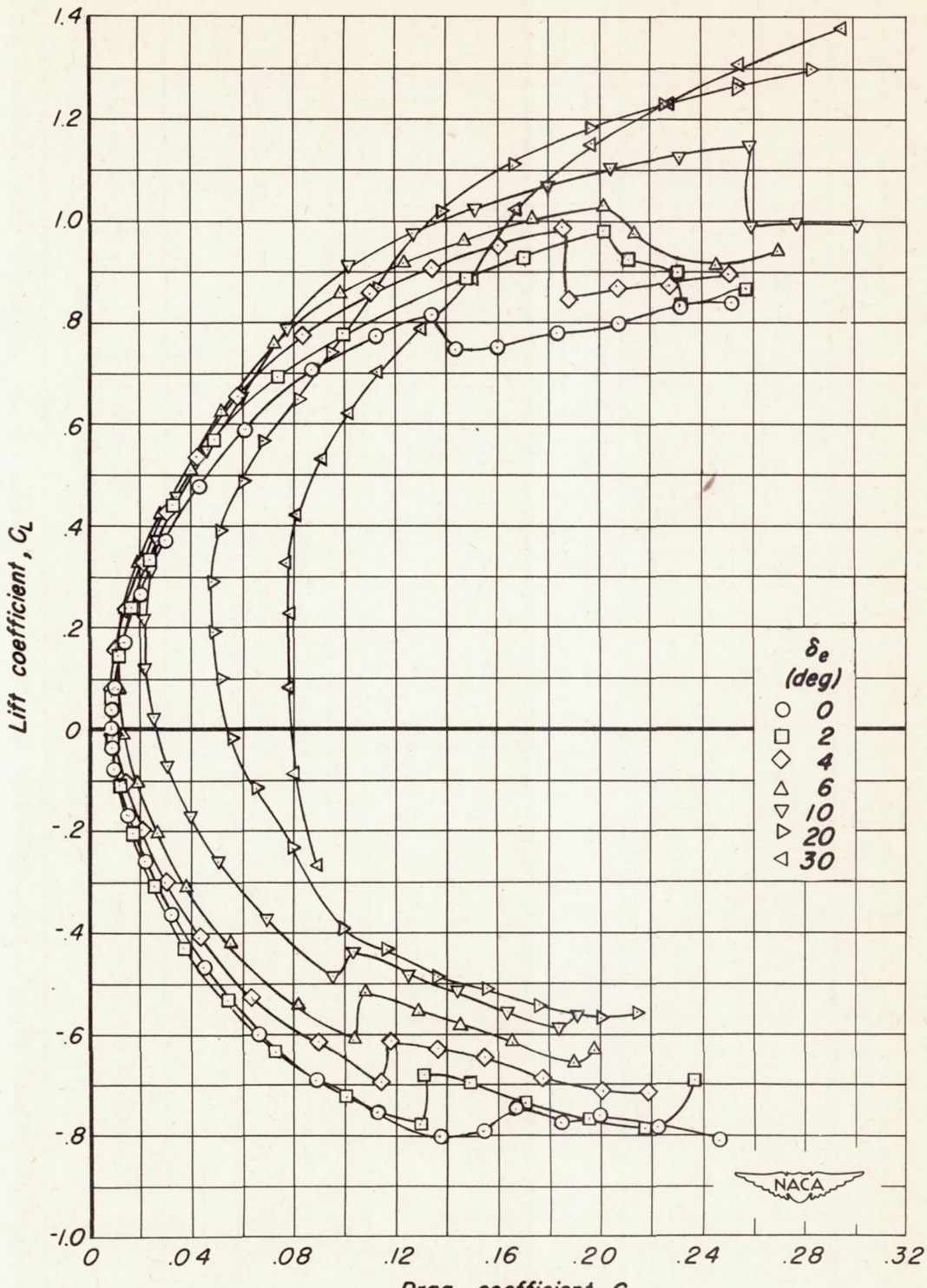

(b) C_L vs C_D.

Figure 7. — Concluded.

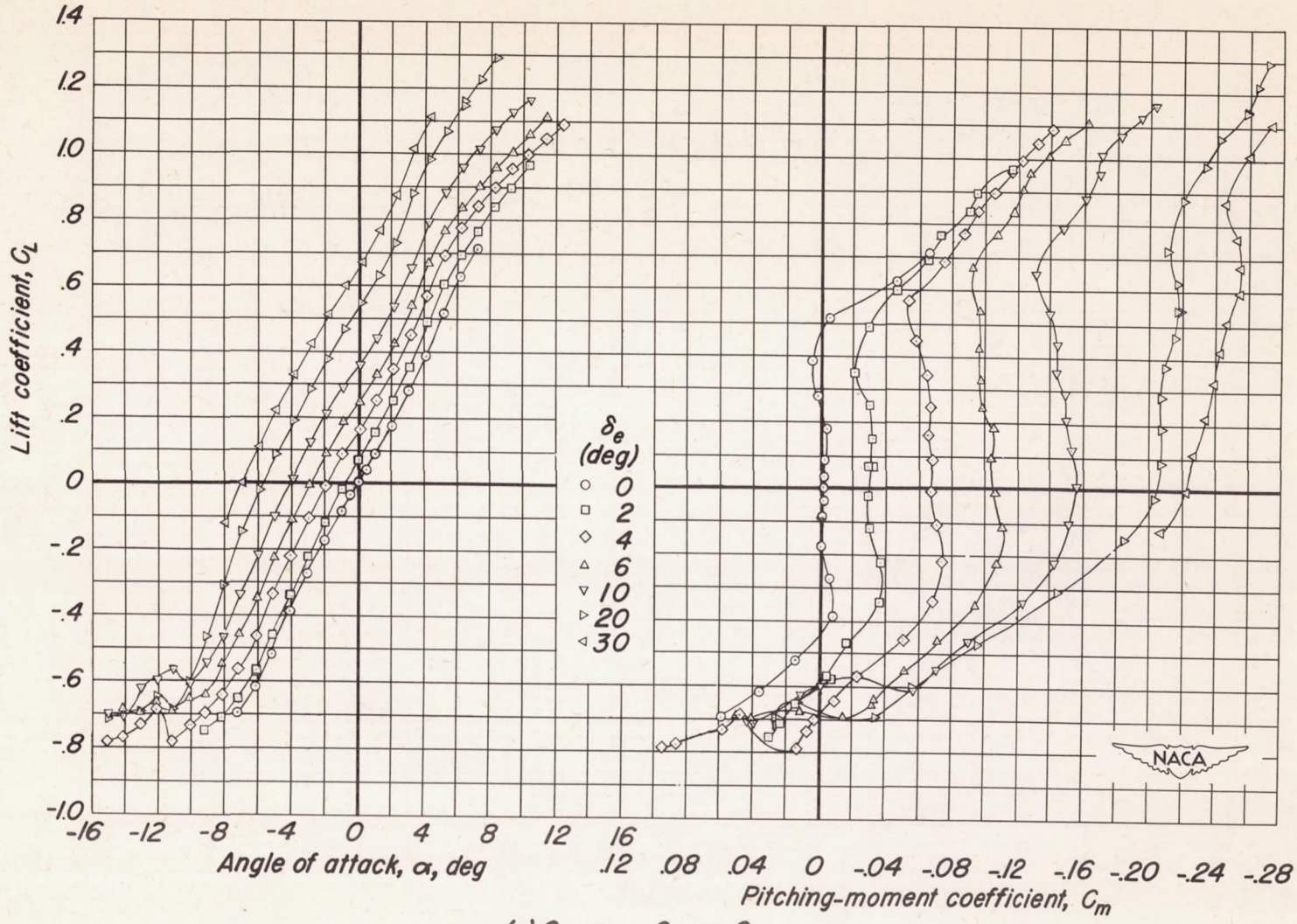

(a) C_L vs α, C_L vs C_m.

Figure 8. — The effect of elevator deflection on the aerodynamic characteristics of the tail at a Mach number of 0.87.

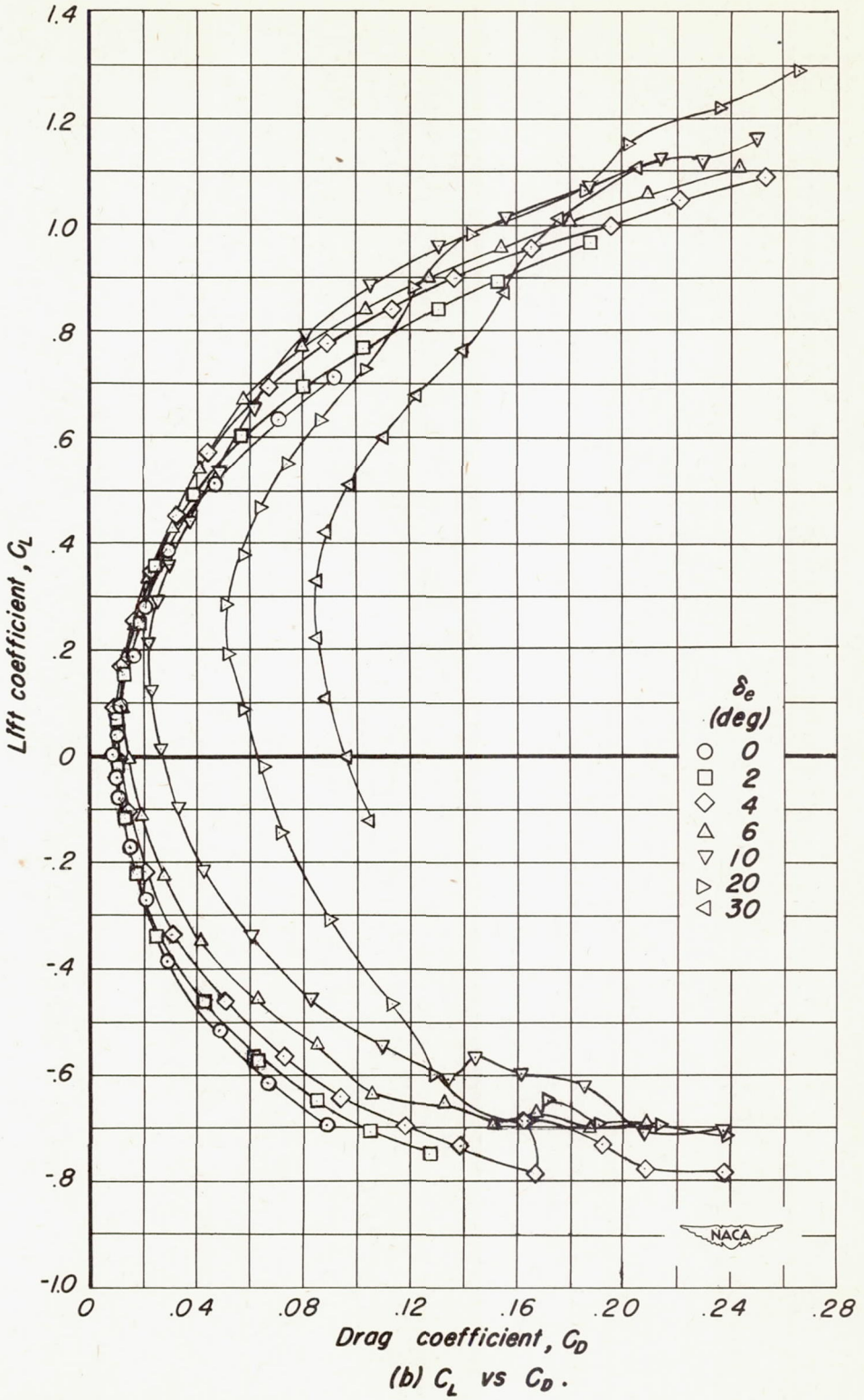

(b) C_L vs C_D.

Figure 8. — Concluded.

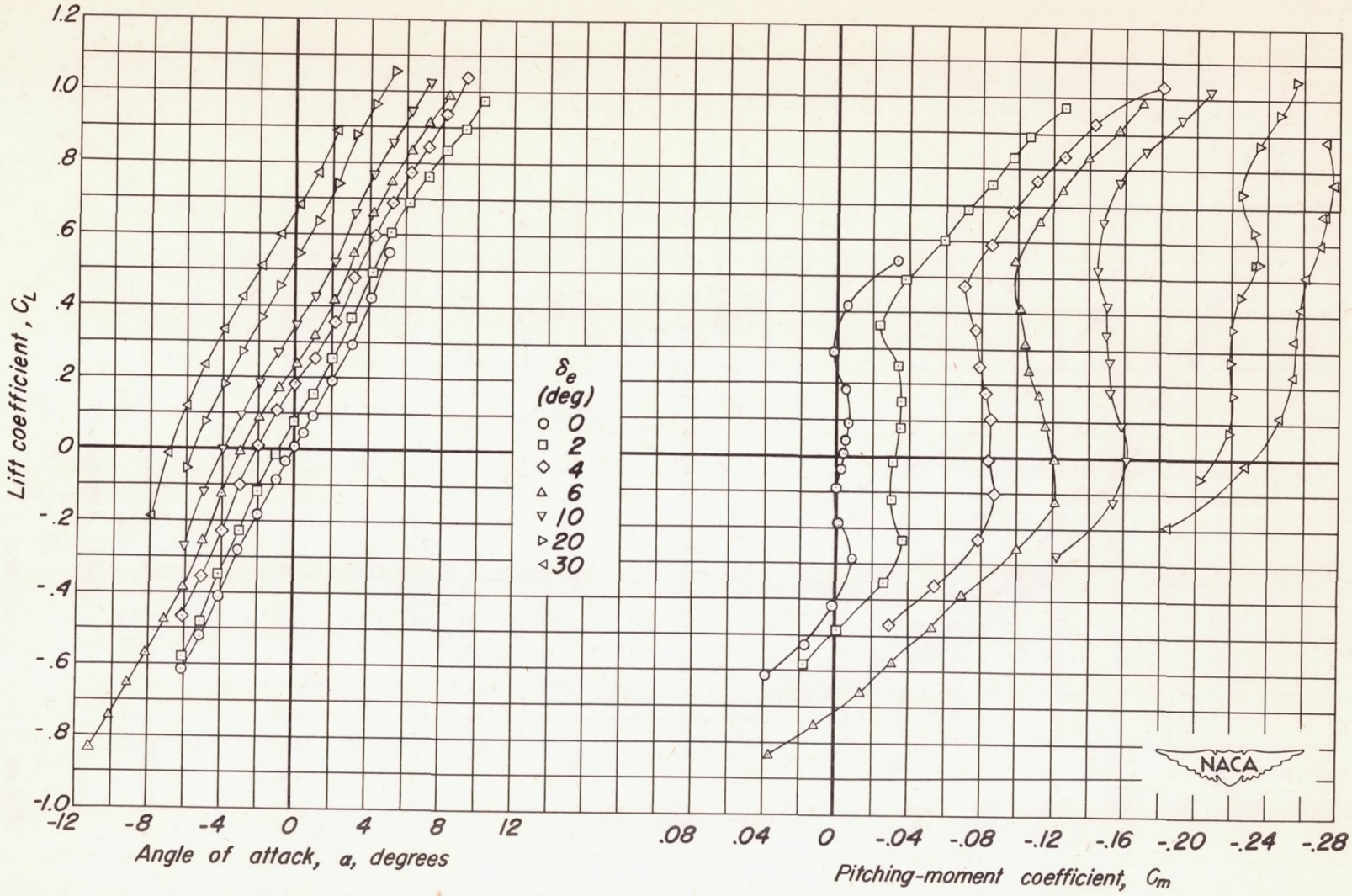

(a) C_L vs α, C_L vs C_m.

Figure 9. — The effect of elevator deflection on the aerodynamic characteristics of the tail at a Mach number of 0.90.

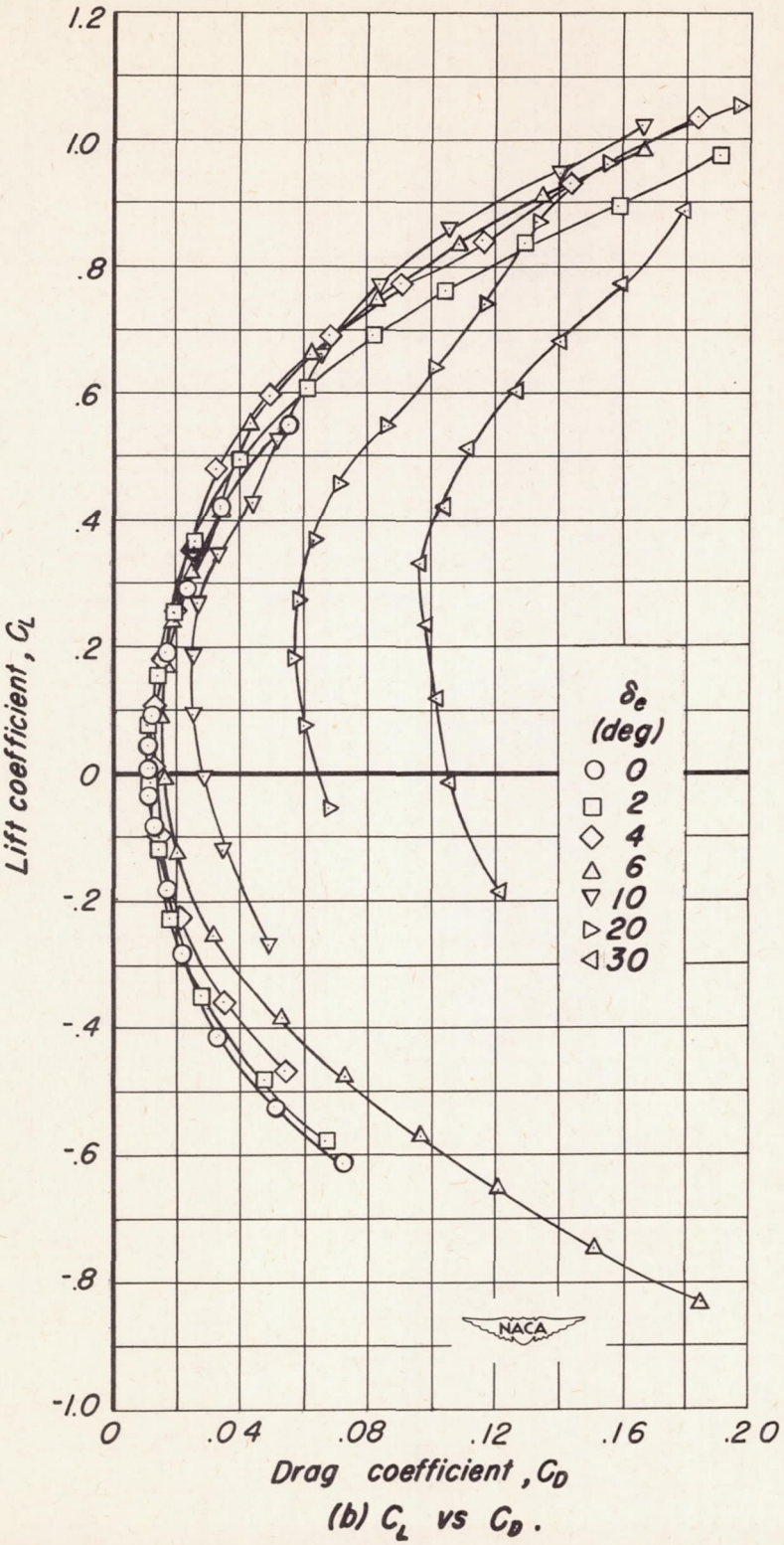

(b) C_L vs C_D.

Figure 9. — Concluded.

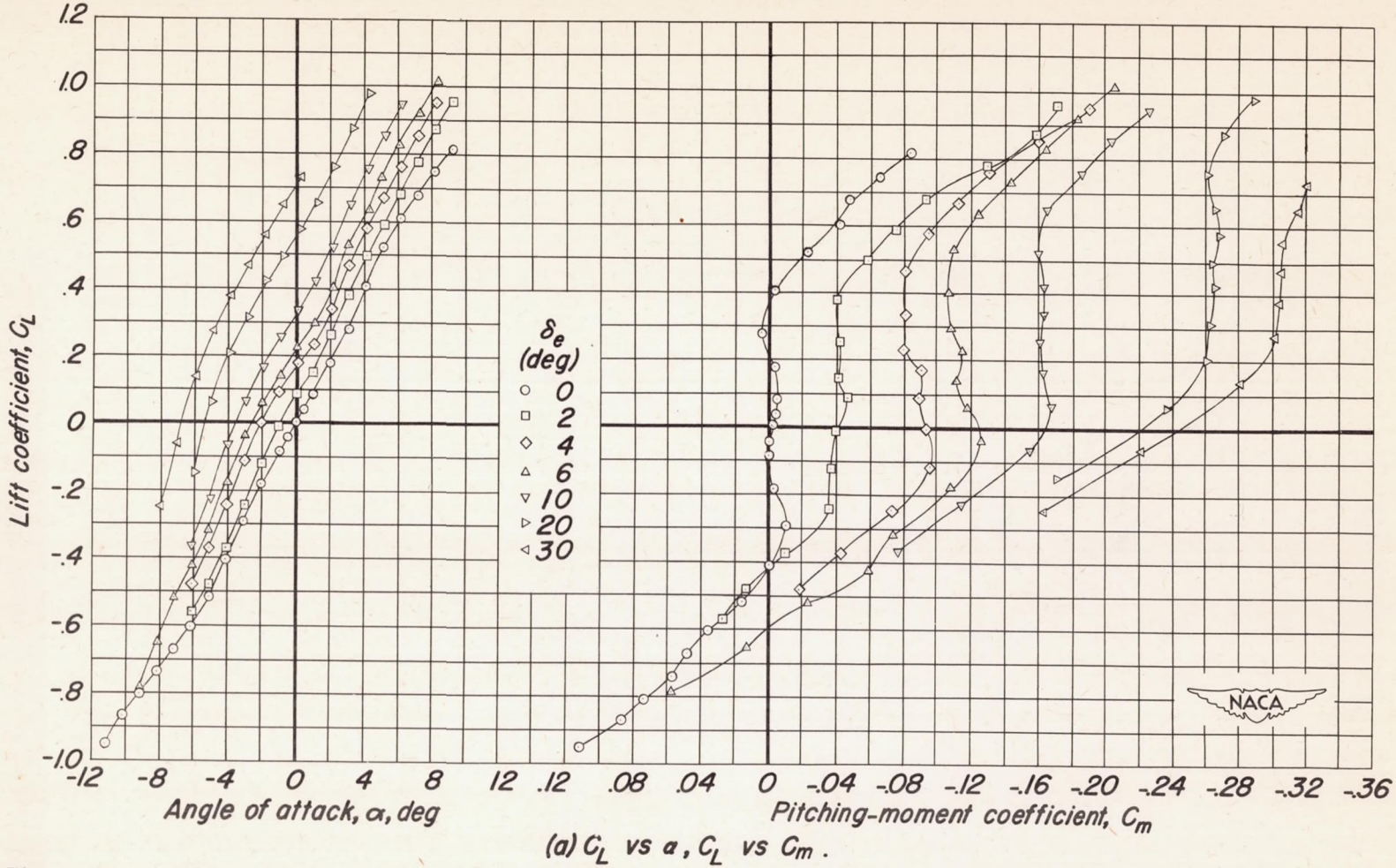

(a) C_L vs α, C_L vs C_m.

Figure 10.— The effect of elevator deflection on the aerodynamic characteristics of the tail at a Mach number of 0.92.

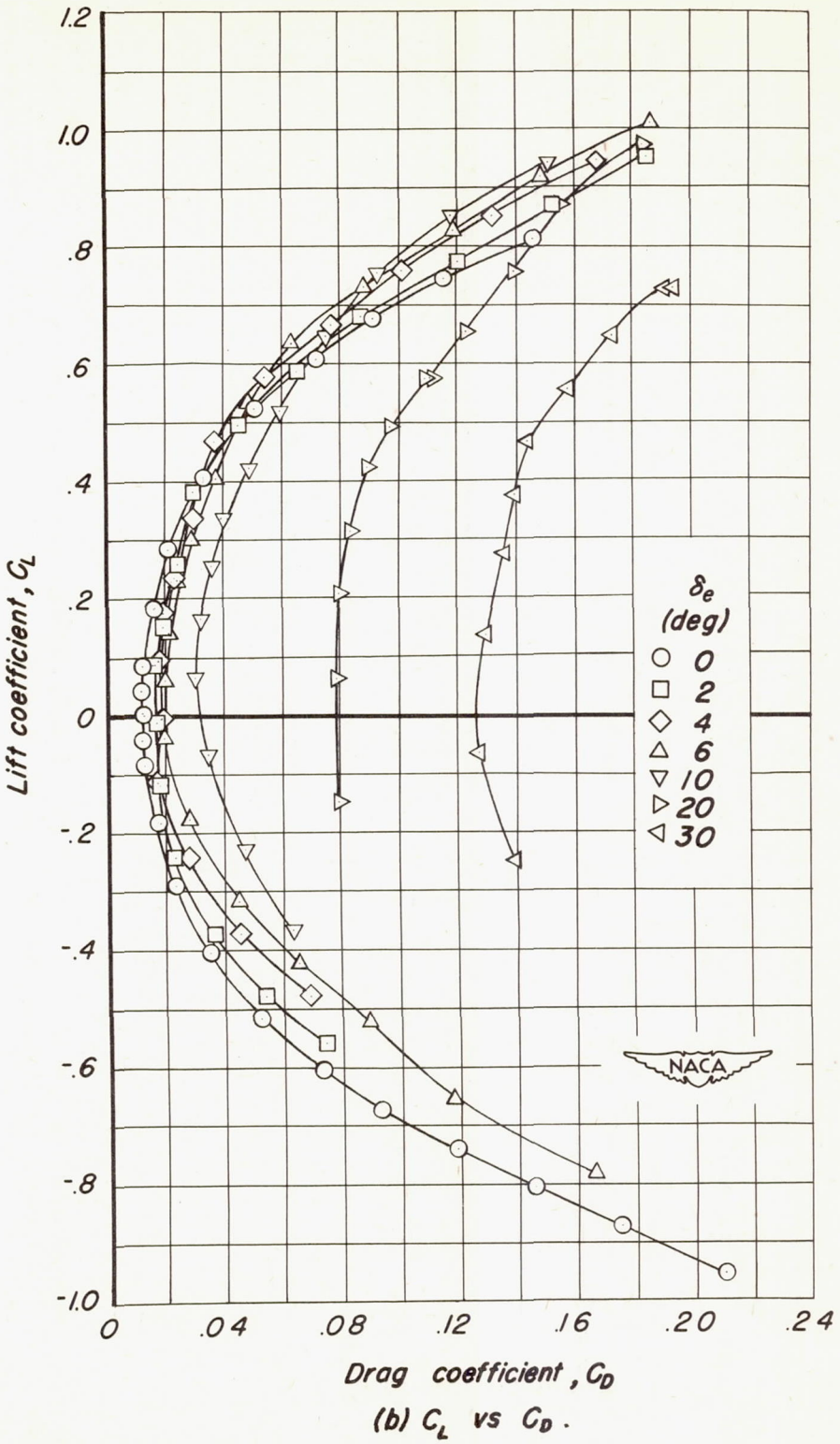

(b) C_L vs C_D.

Figure 10. — Concluded.

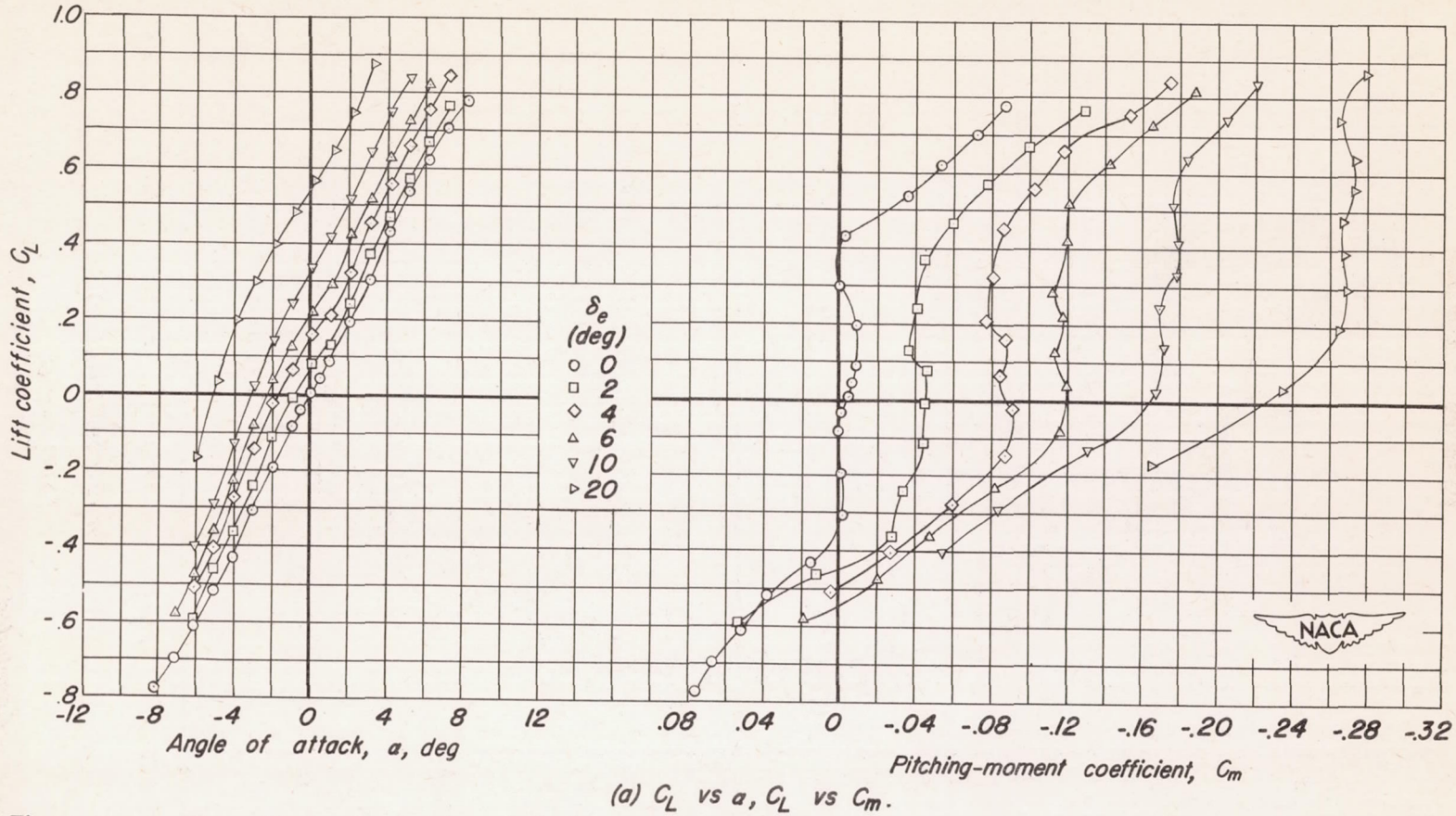

(a) C_L vs a, C_L vs C_m.

Figure 11. — The effect of elevator deflection on the aerodynamic characteristics of the tail at a Mach number of 0.94.

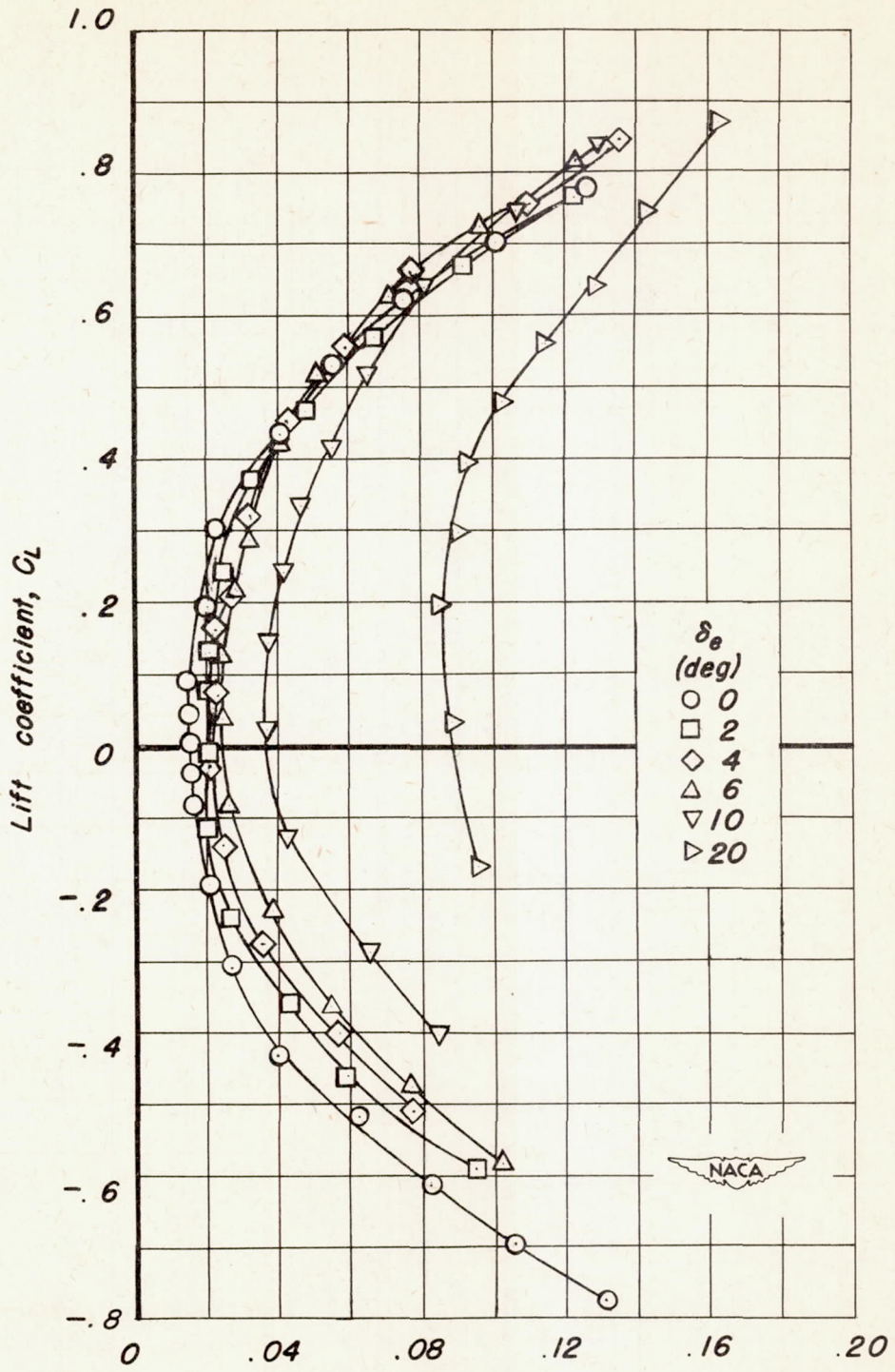

(b) C_L vs C_D.

Figure 11.- Concluded.

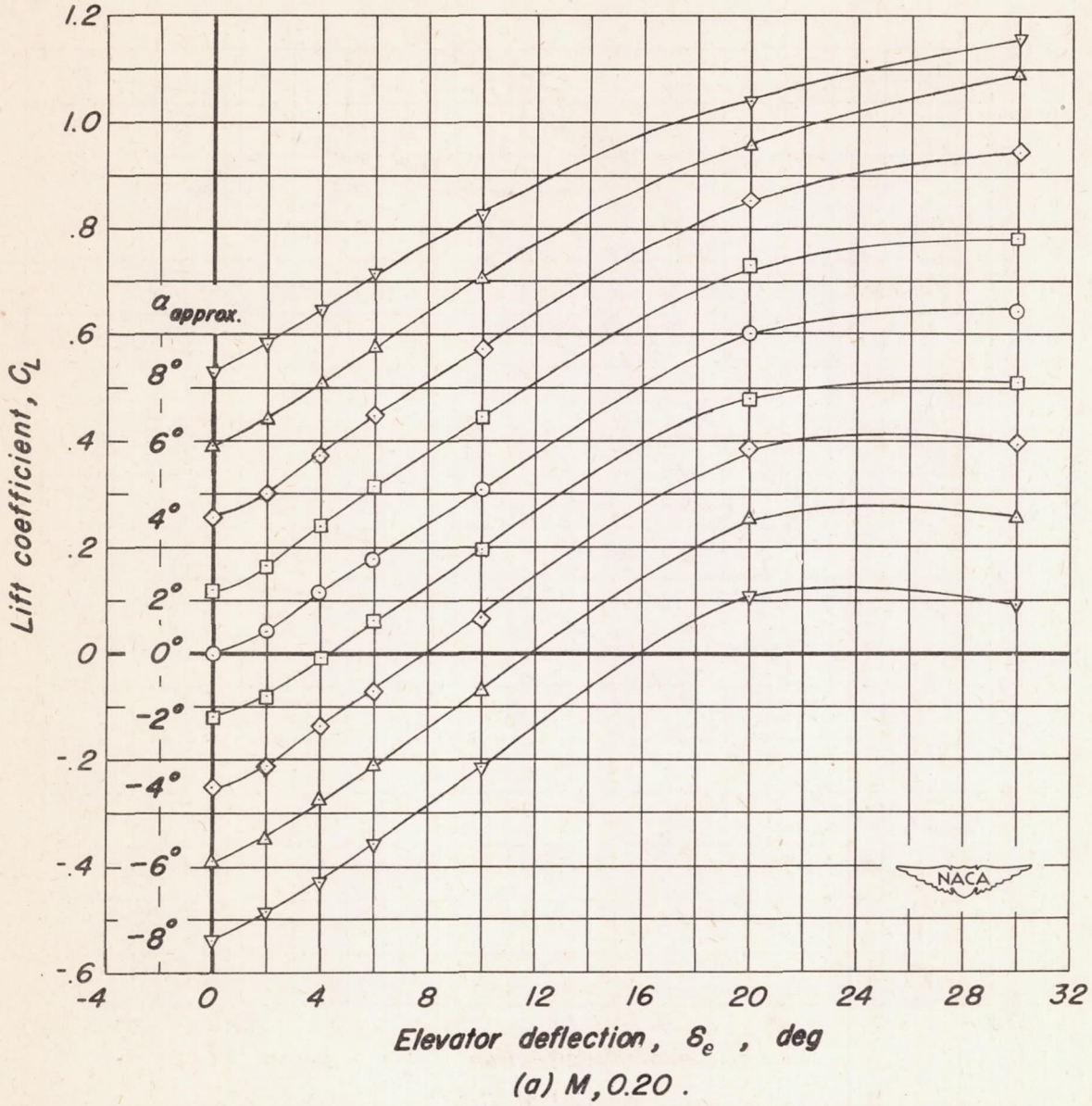

(a) M, 0.20 .

Figure 12.——The variation of lift coefficient with elevator deflection for various angles of attack of the tail .

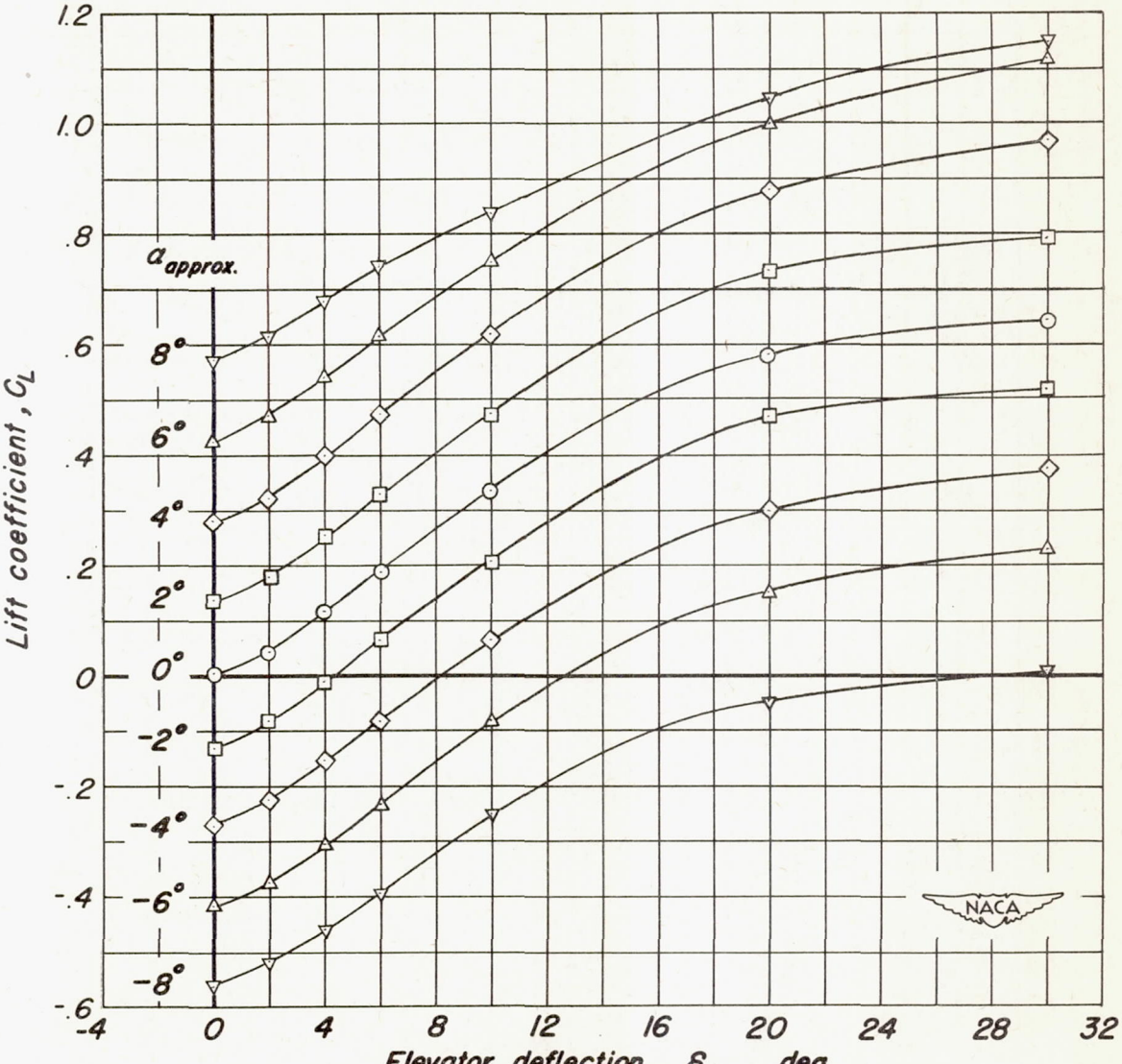

(b) M, 0.50.

Figure 12. — Continued.

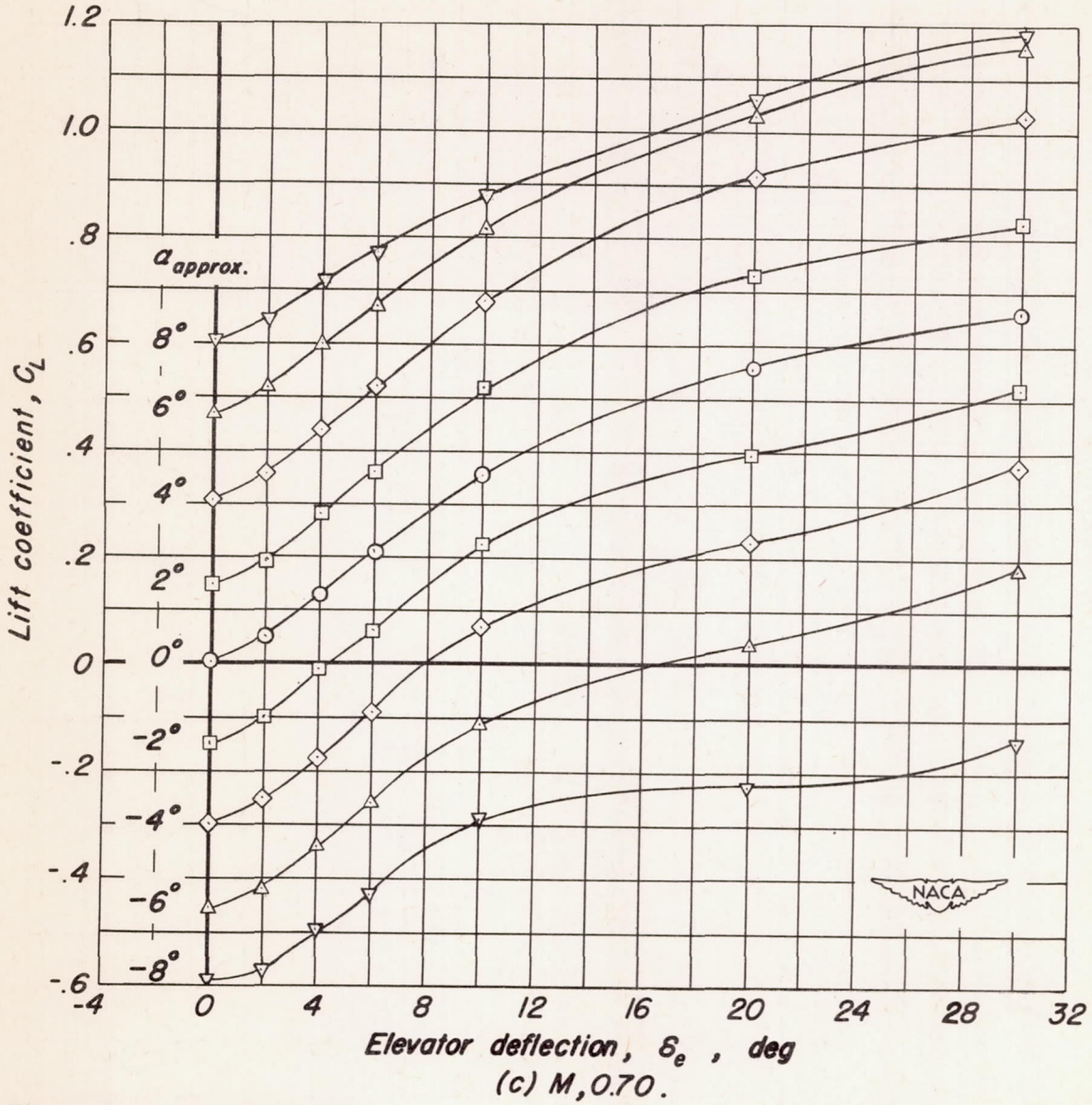

(c) M, 0.70.

Figure 12. — Continued.

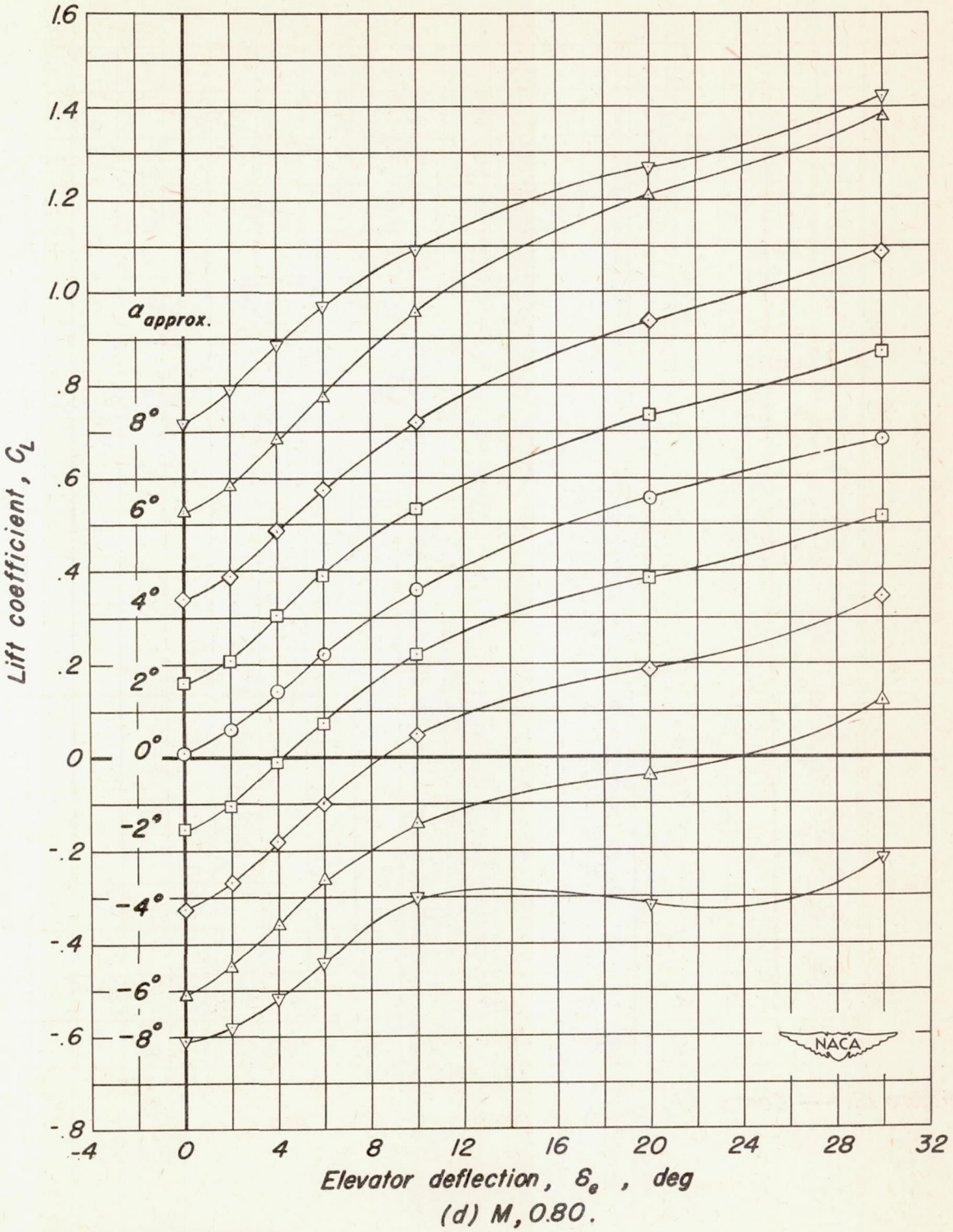

(d) M, 0.80.

Figure 12. — Continued .

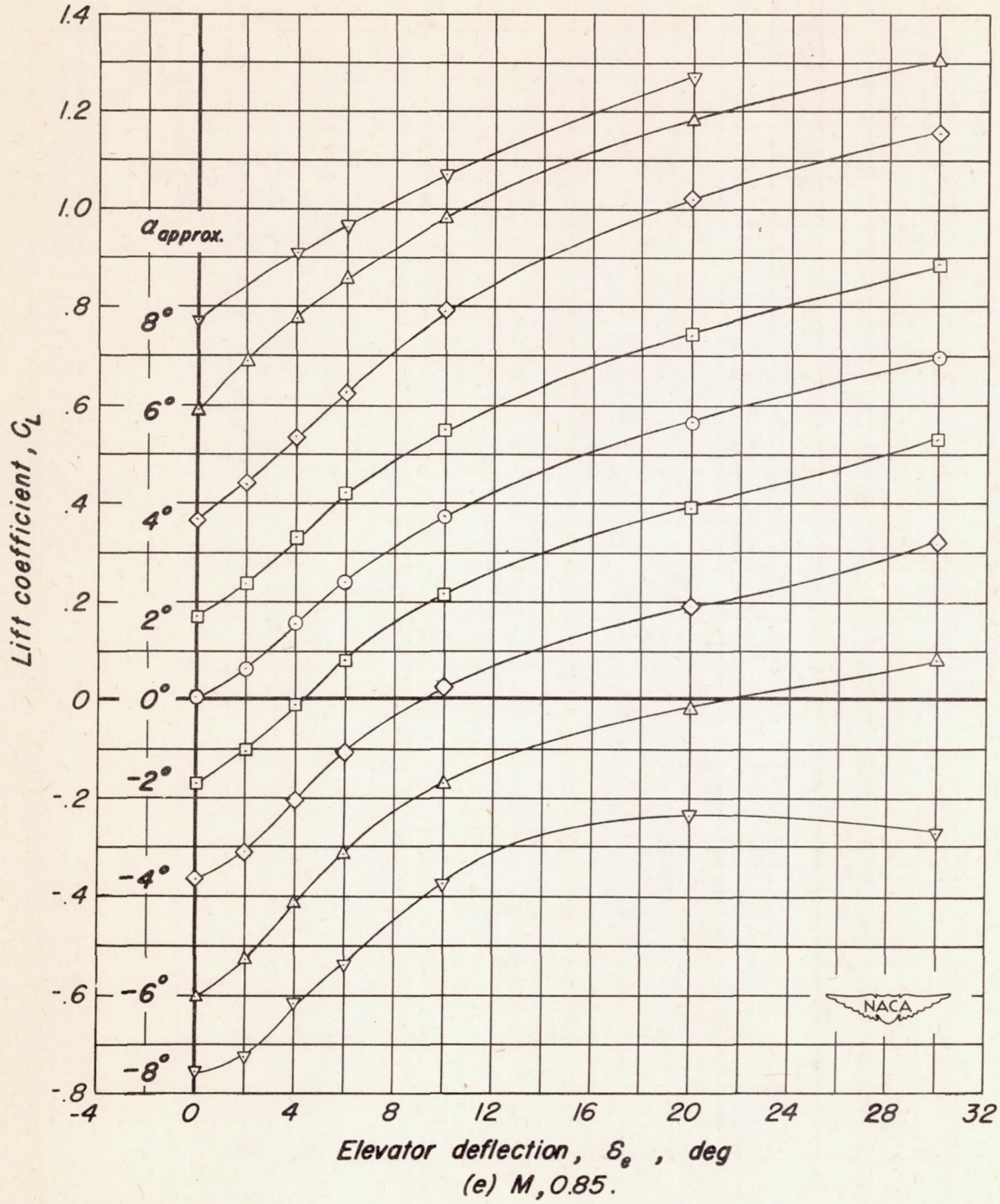

(e) M, 0.85.

Figure 12. — Continued .

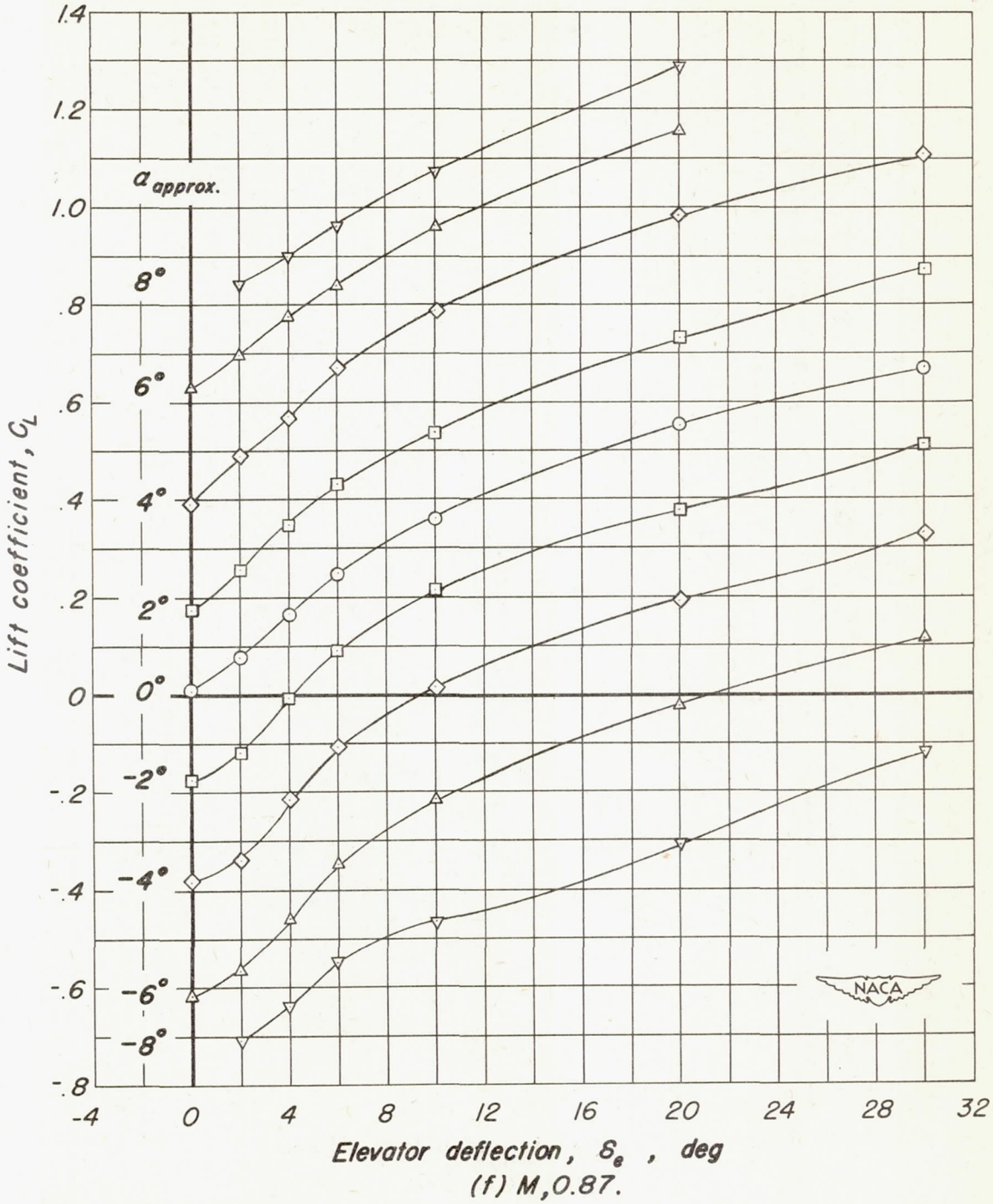

(f) M,0.87.

Figure 12. — Continued .

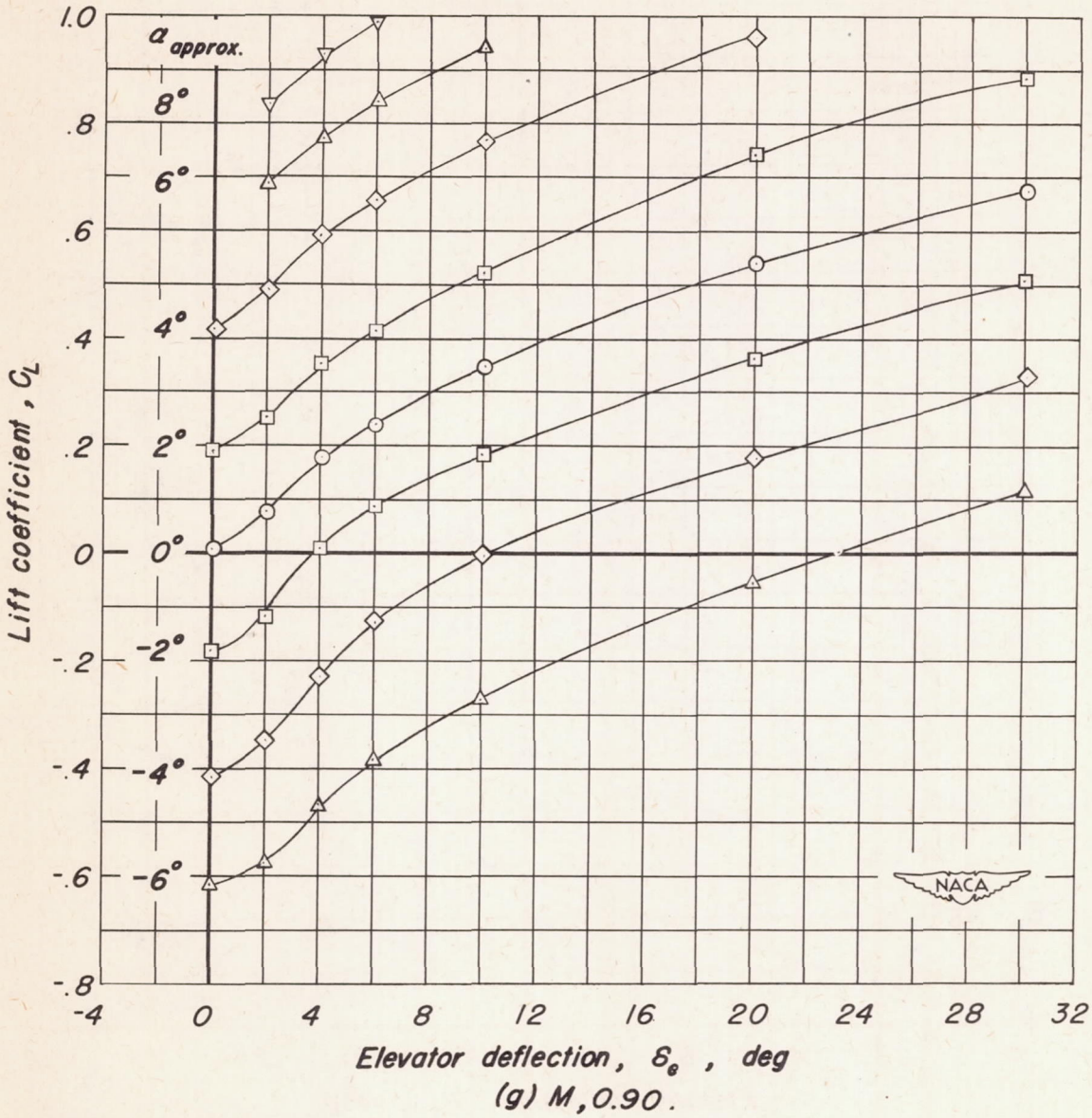

(g) M, 0.90.

Figure 12. — Continued.

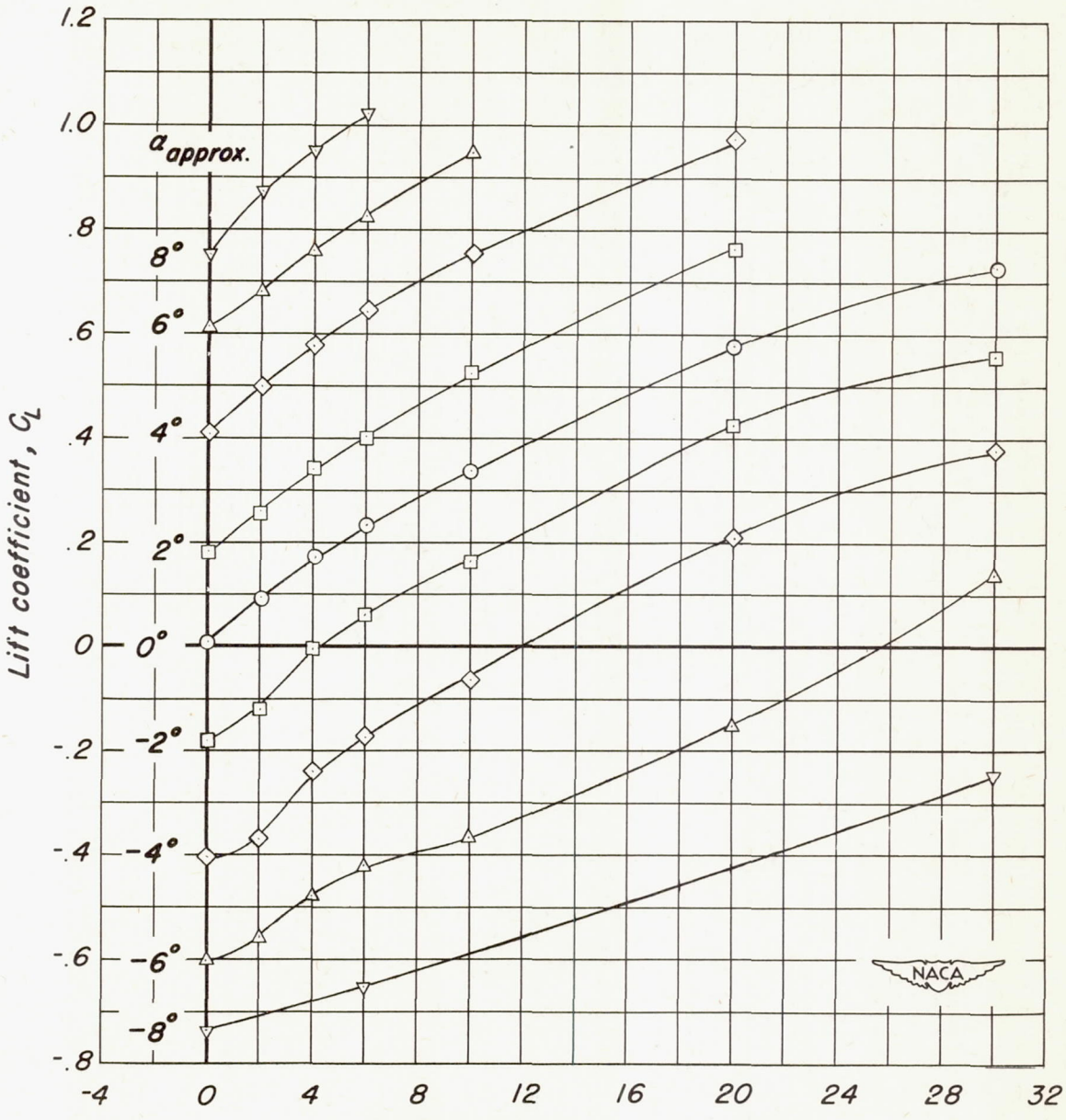

(h) M,0.92.

Figure 12. — Continued.

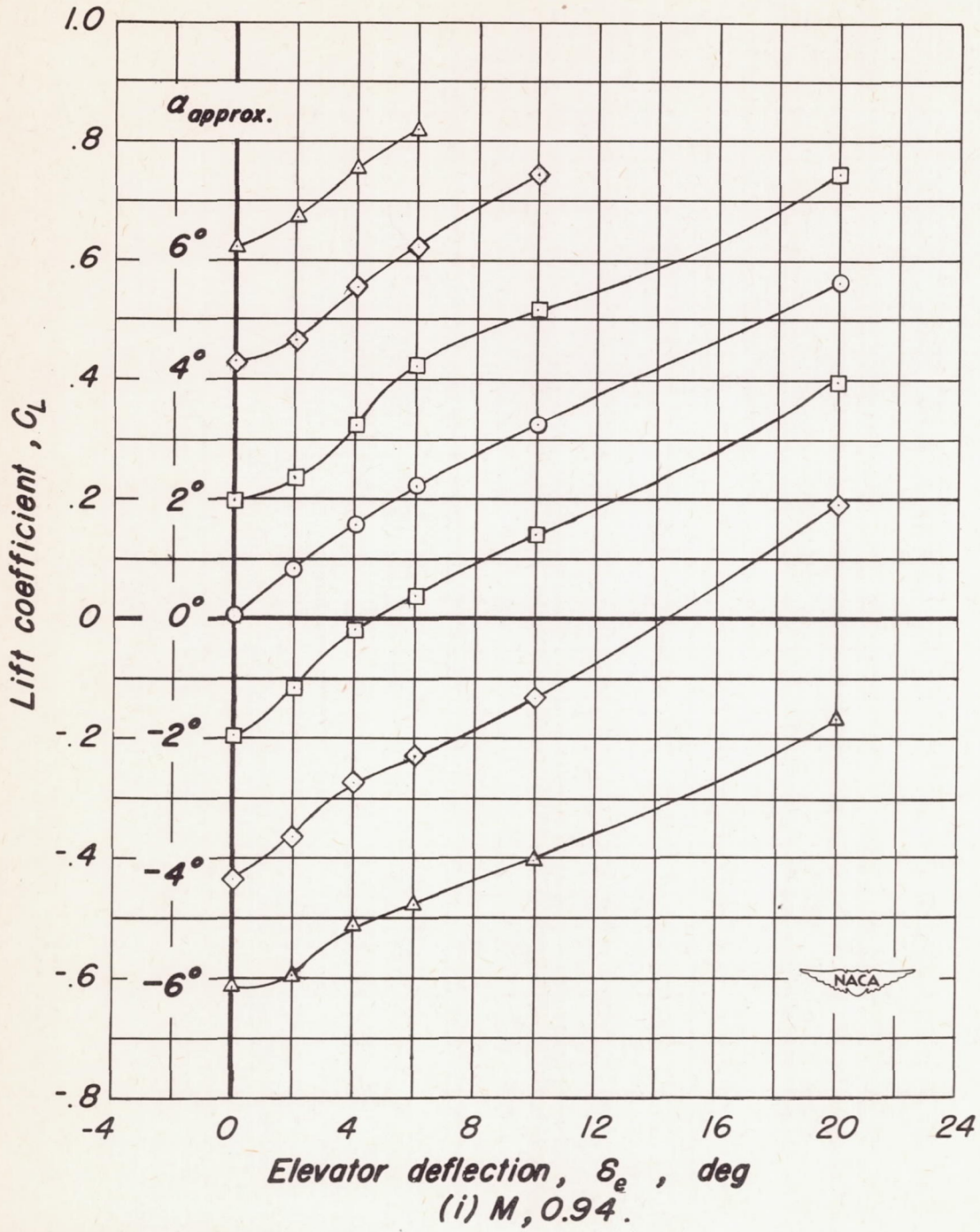

(i) M, 0.94.

Figure 12.— Concluded.

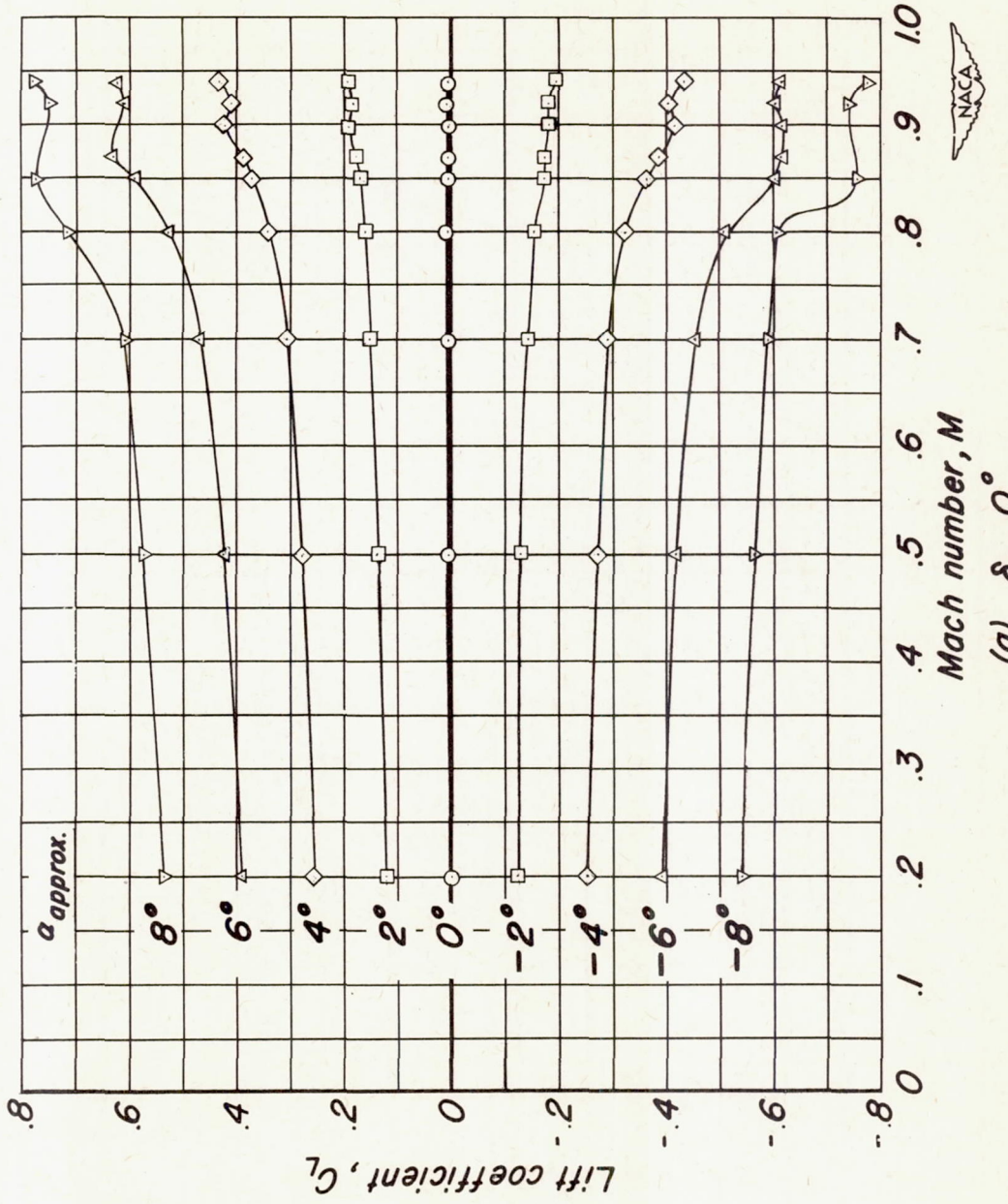

(a) δ_e, 0°.

Figure 13.— The variation of lift coefficient with Mach number for various angles of attack of the tail.

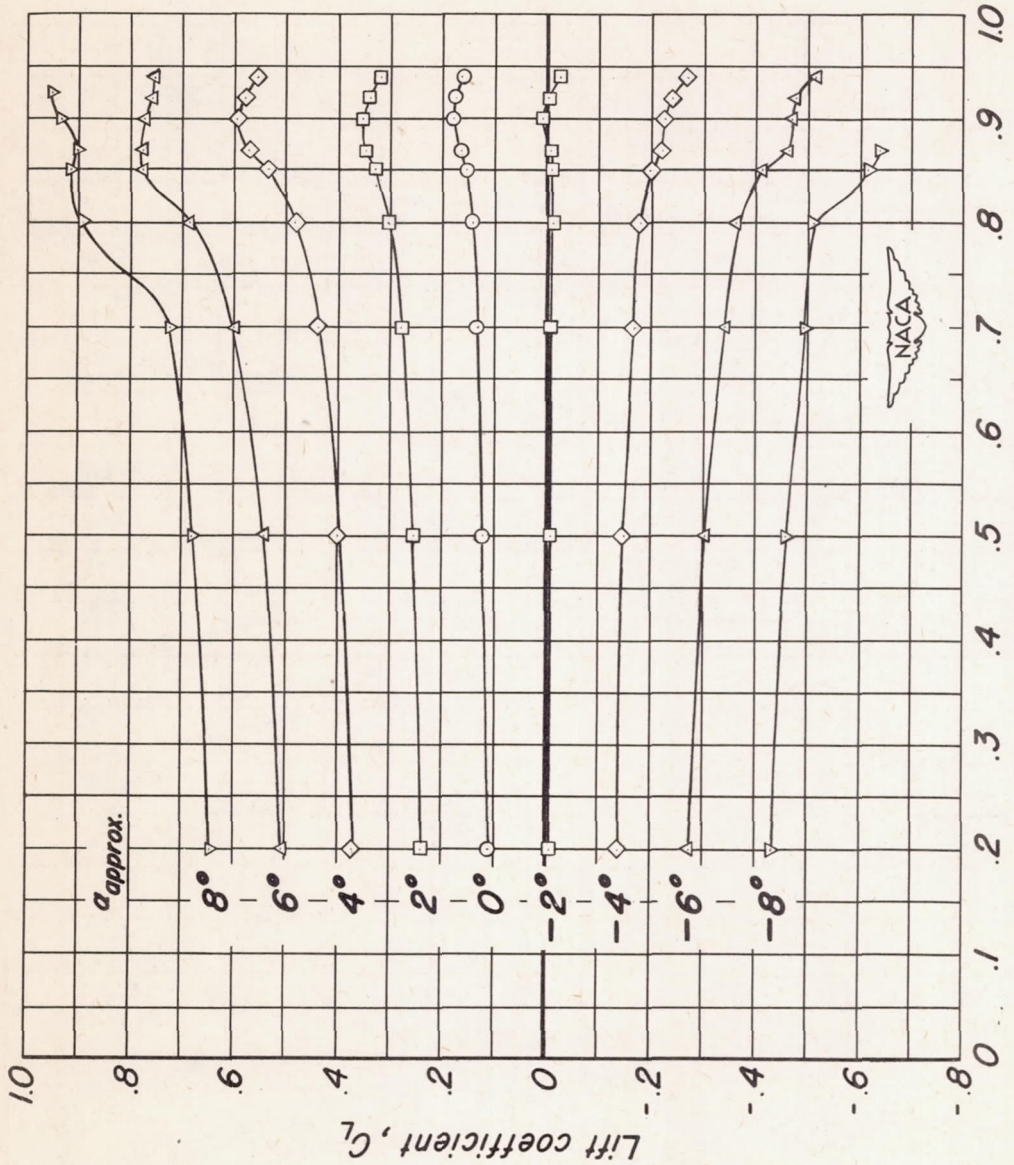

(b) δ_e, 4°.

Figure 13.— Continued.

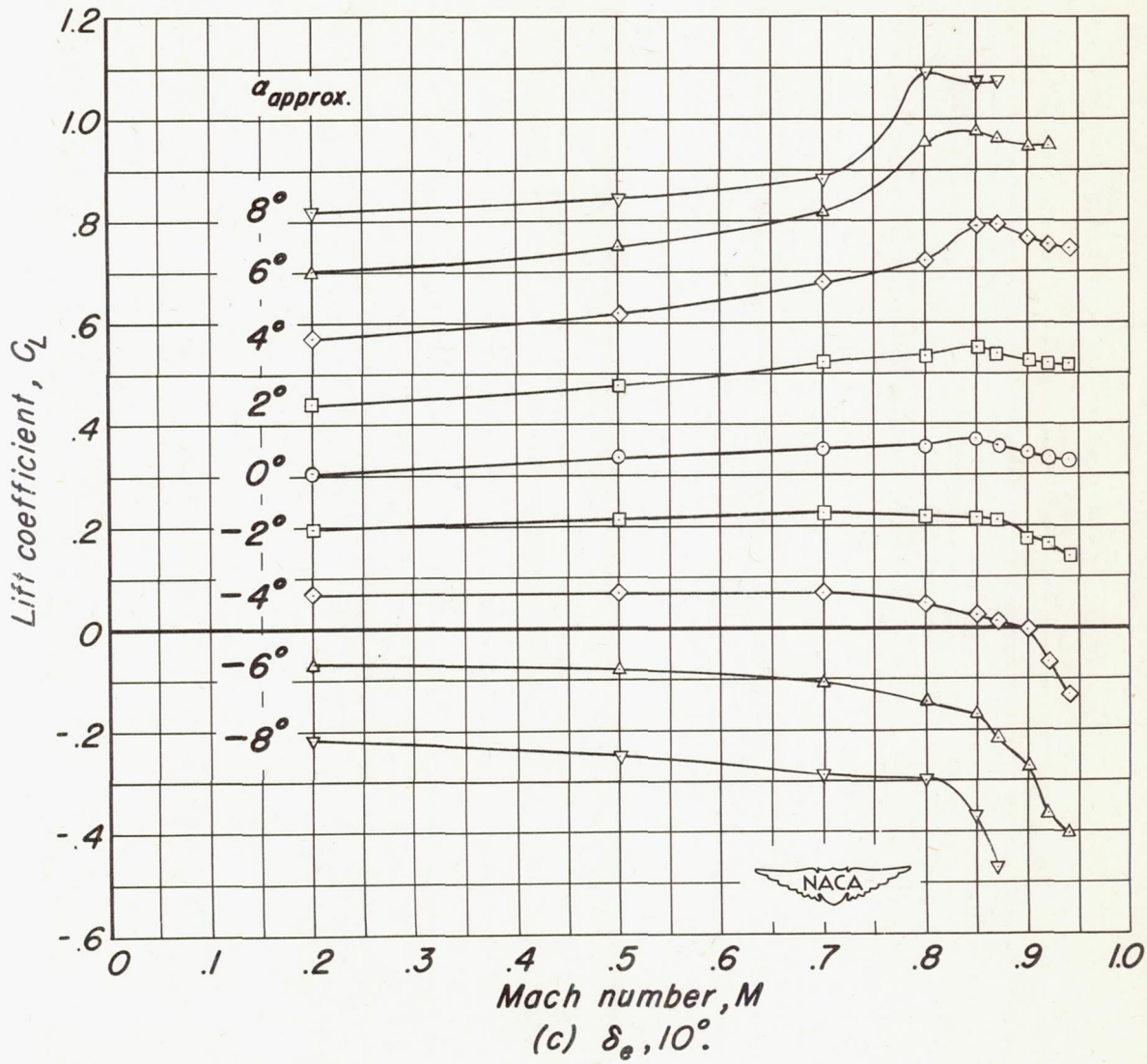

(c) δ_e, 10°.

Figure 13.— Continued.

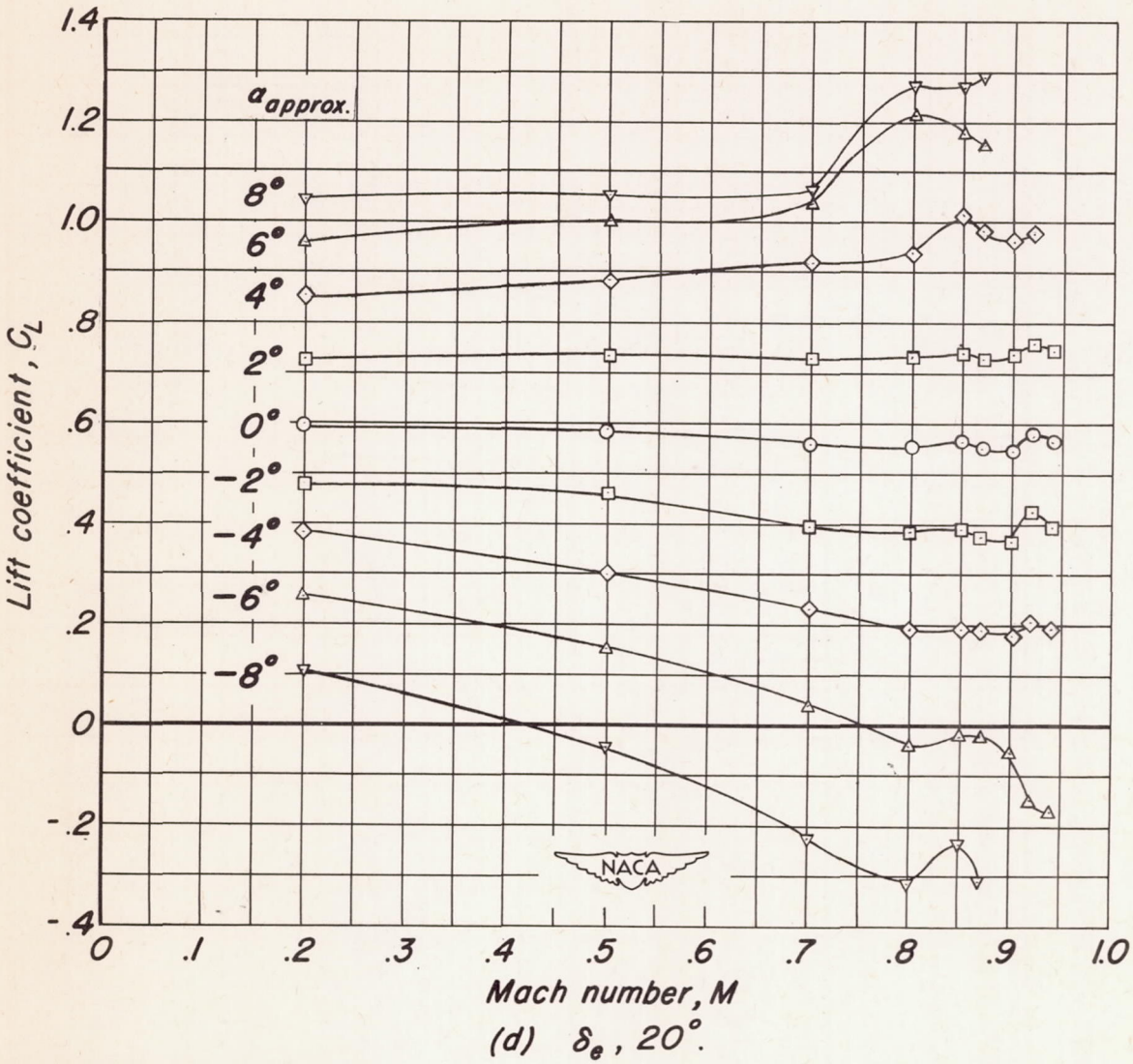

(d) δ_e, 20°.

Figure 13.— Continued.

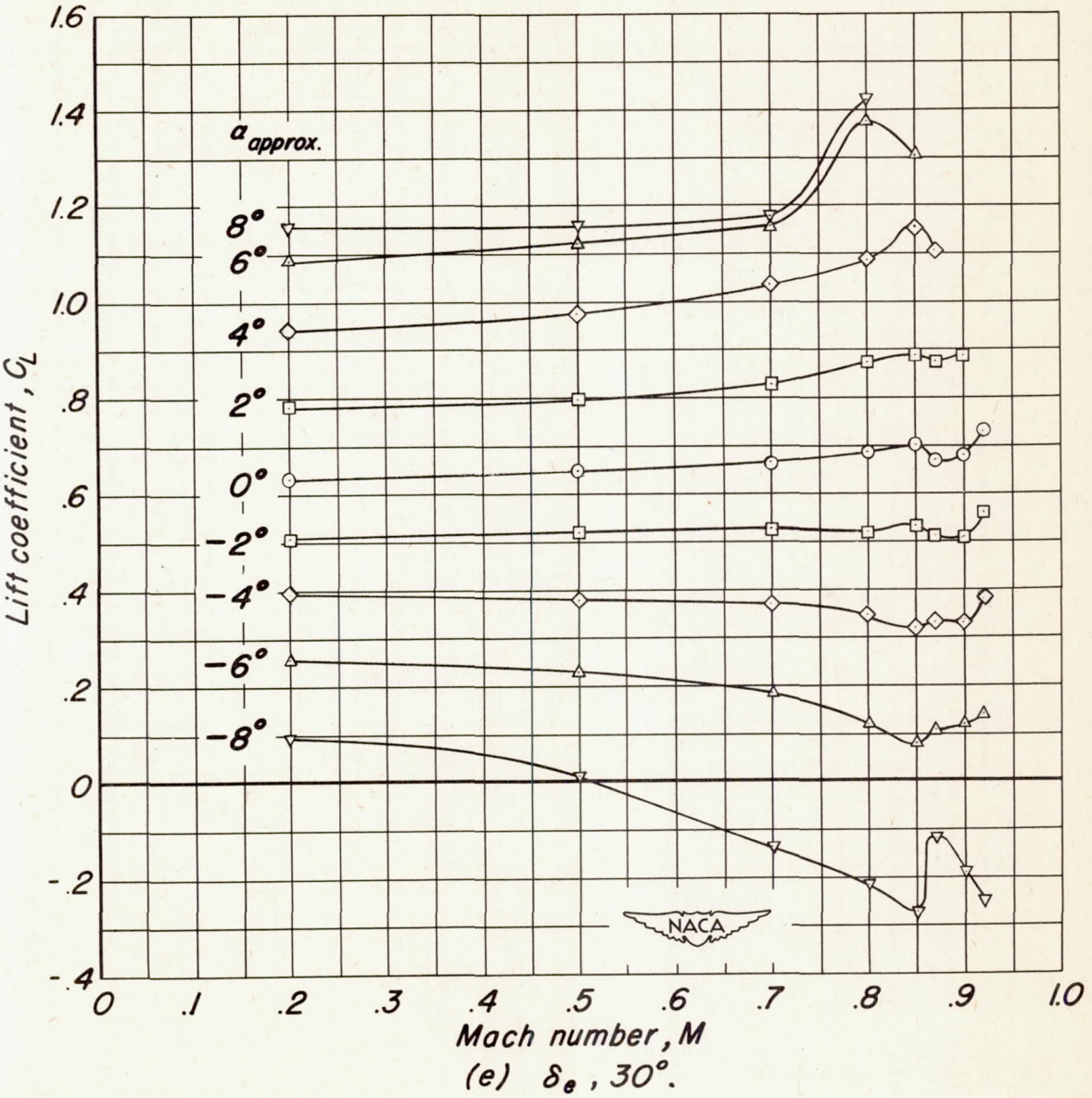

(e) δ_e, 30°.

Figure 13. — Concluded.

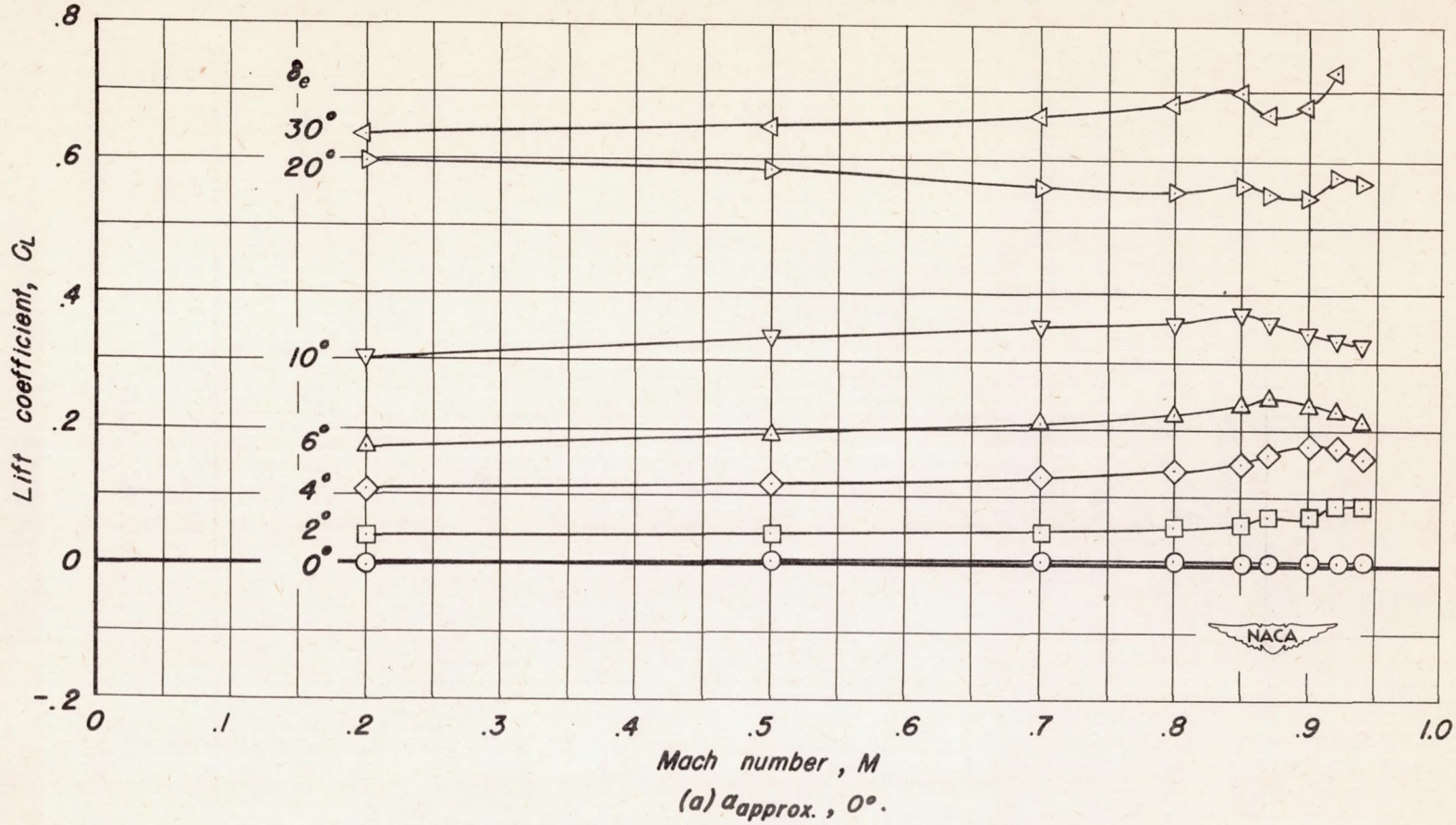

(a) $\alpha_{approx.}$, 0°.

Figure 14.—The variation of lift coefficient with Mach number for various elevator deflections.

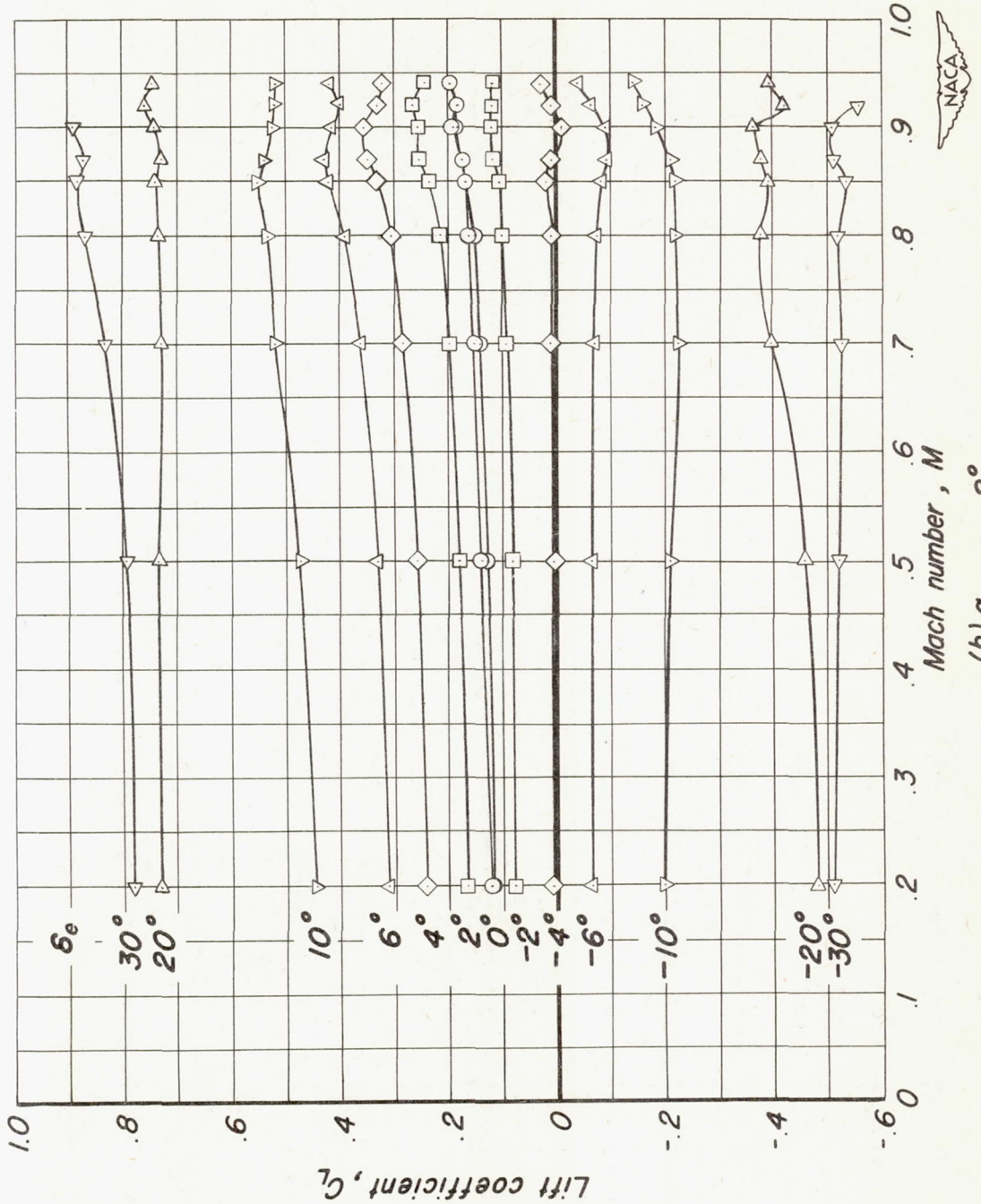

(b) $\alpha_{approx.}$, 2°.

Figure 14.— Continued.

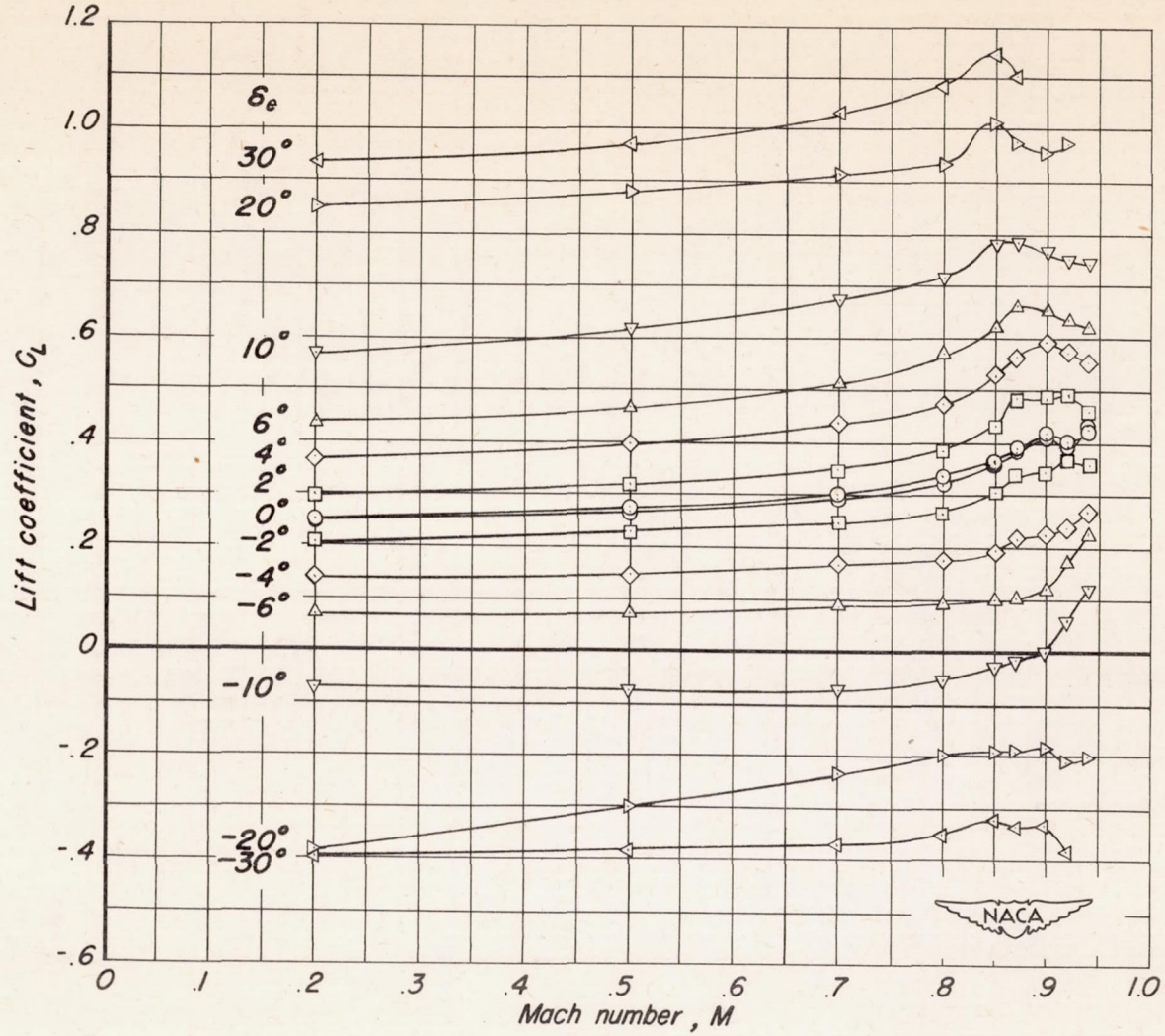

(c) $\alpha_{approx.}$, 4°.

Figure 14.— Continued.

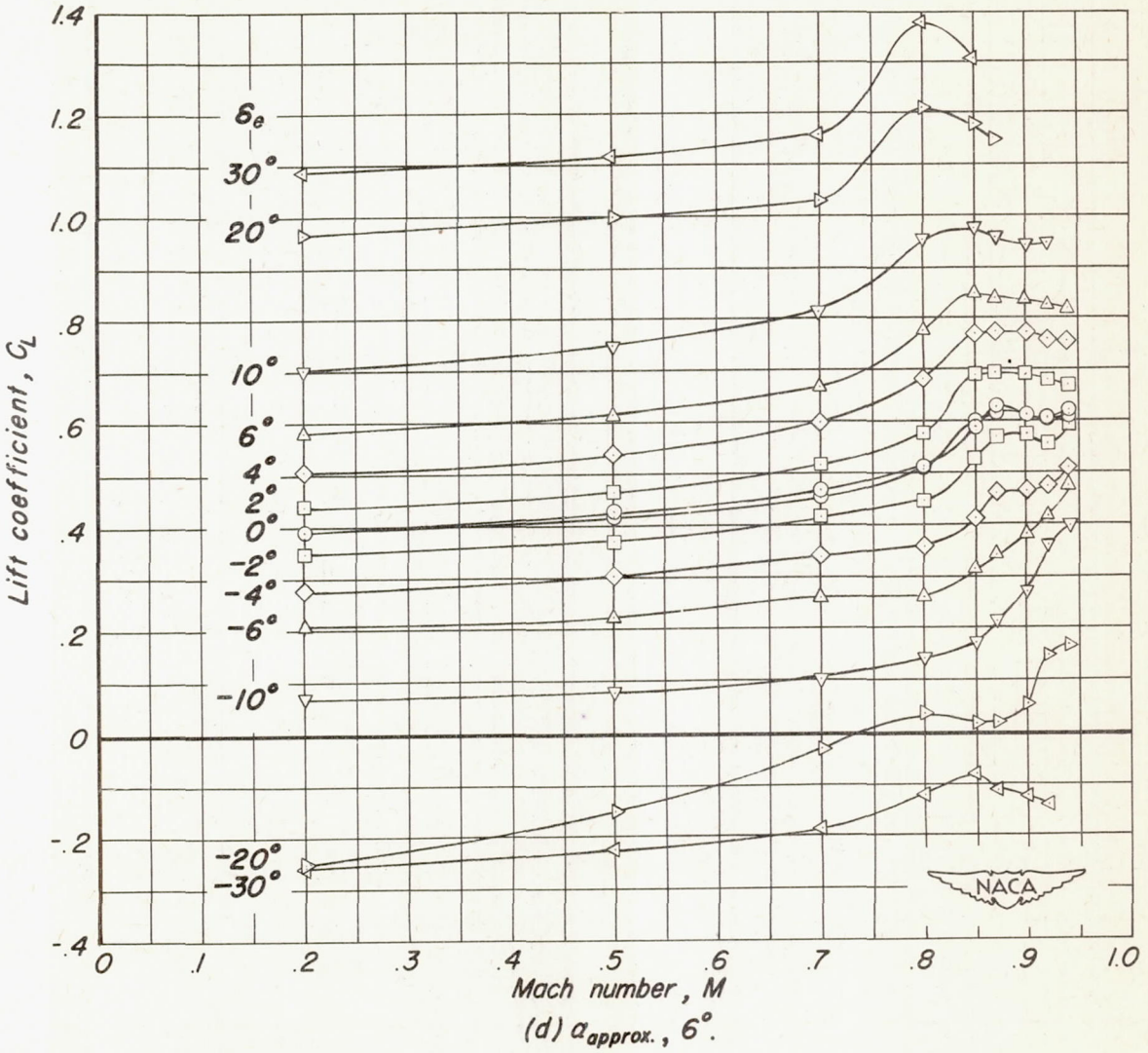

Figure 14.— Continued.

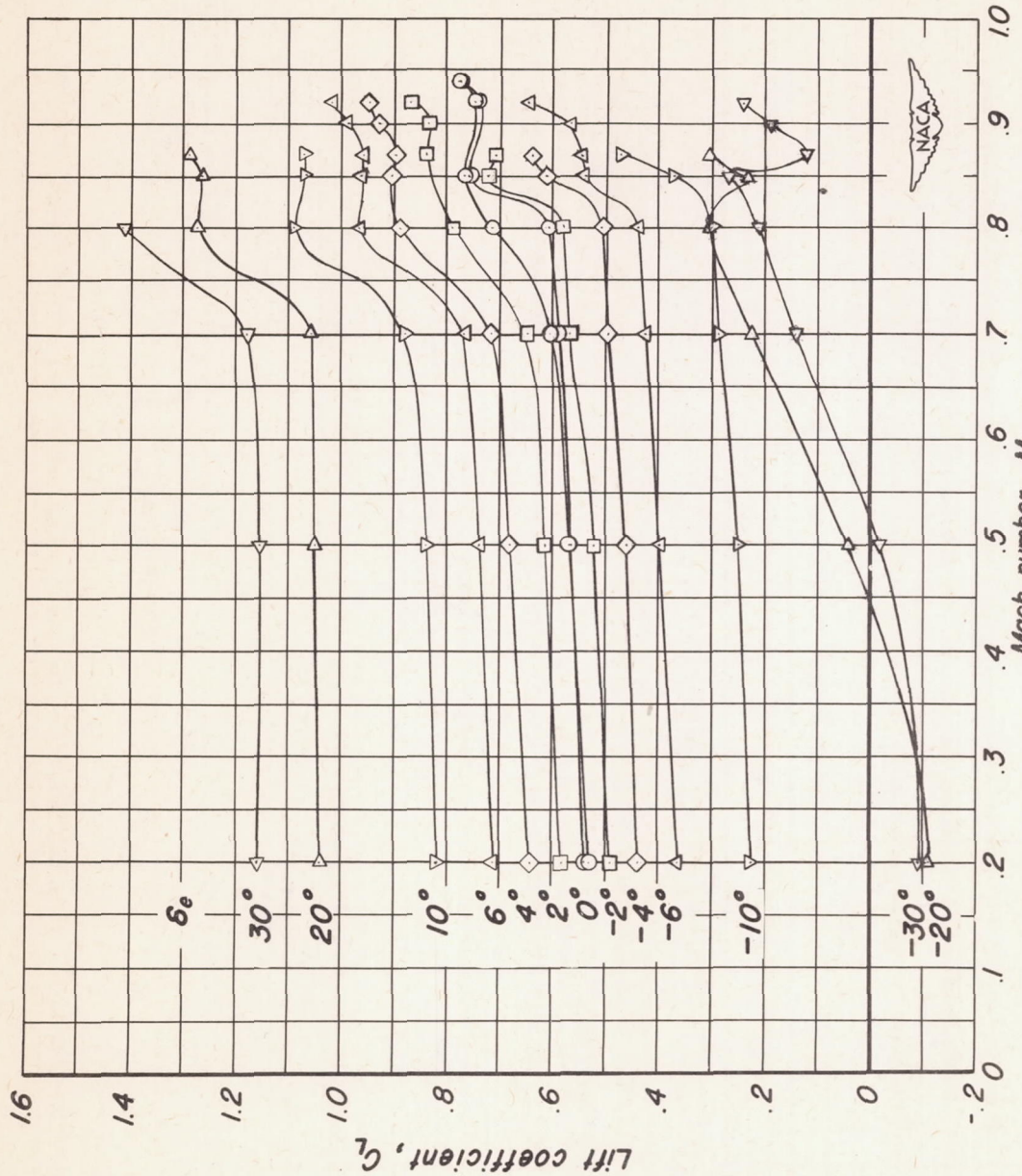

Figure 14.—Concluded.

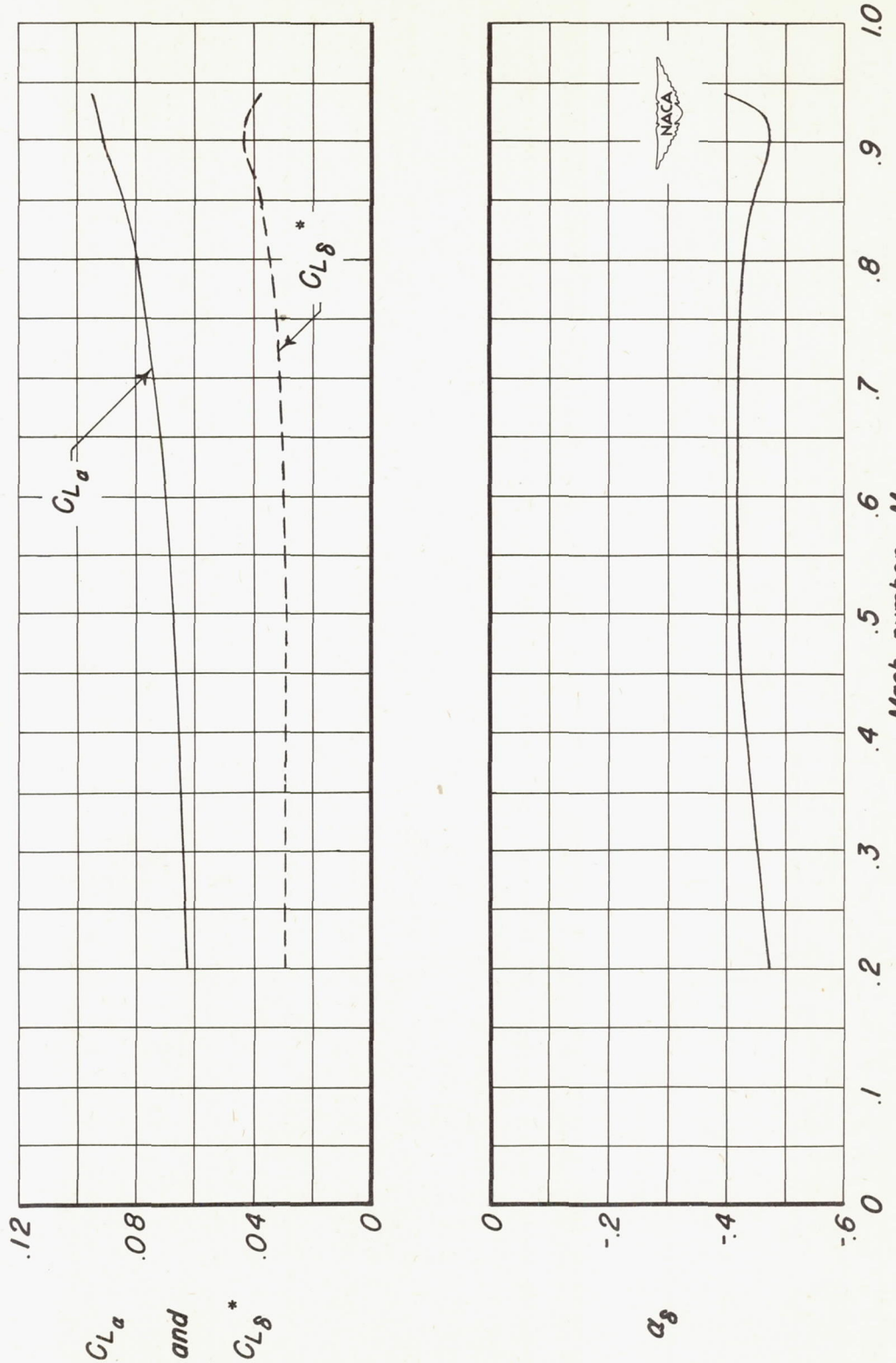

Figure 15.— Variation of lift parameters C_{L_α}, $C_{L_\delta}^*$, and α_δ with Mach number.